Structure-Reactivity Relationship for Titania Supported Chromium-Phosphorus-Oxide catalysts: ODH of Propane

By

Priyanka Singh

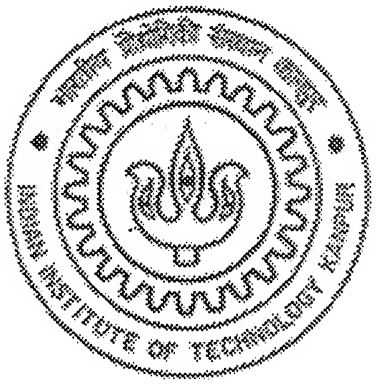

DEPARTMENT OF CHEMICAL ENGINEERING

INDIAN INSTITUTE OF TECHNOLOGY, KANPUR

April, 2004

Structure-Reactivity Relationship for Titania Supported Chromium-Phosphorus-Oxide catalysts: ODH of Propane

A thesis submitted in Partial Fulfillment of the

Requirements for the Degree of

Master of Technology

By

Priyanka Singh

to the

Department of Chemical Engineering

Indian Institute of Technology, Kanpur, INDIA

April, 2004

Dedicated

To

My

Late **Brother**

CERTIFICATE

It is certified that the work contained in the thesis entitled *"Structure-Reactivity Relationship for Titania Supported Chromium-Phosphorus-Oxide catalysts: ODH of Propane"* by Priyanka Singh, has been carried out under my supervision and that this work has not been submitted elsewhere for a degree.

Dr. Goutam Deo
Associate Professor
Department of Chemical Engineering
Indian Institute of Technology Kanpur
Kanpur INDIA
April 2004

Acknowledgements

I would like to express my deep gratitude towards my thesis supervisor, Dr. Goutam Deo for his guidance, co-operation, encouragement and patience through out my thesis work. I thank him for providing me all the requisites for the completion of my work. Besides being an excellent supervisor, Dr. Deo is a very nice person too. I cherish the times that I spent with him as my supervisor.

I would like to extend my thanks to Dr. D. Kunzru for allowing me to use the TPR apparatus in his lab.

I am also thankful to Mr. Umashankar and Mr. Sharma of ACMS and Mr. Kanojiaji of EPR lab for their help and a note of thanks to Hemanta (lab assistant).

I thank my Lab mates Kamala, Mallesh, Rudra, Debaprasad and Girish for all the help they rendered to me through out my thesis work. Thanks to Maymol, Mahuya and Veena for their timely help.

Above all, I am deeply indebted to all my family members for their constant support, love and encouragement.

Priyanka Singh

Contents

List of Tables

List of Figures

ABSTRACT

The effect of phosphorus as a modifier on titania supported chromium oxide was studied for the oxidative dehydrogenation (ODH) of propane. A series of catalysts of unmodified and phosphorus modified chromia/titania in three different chromium to phosphorus molar ratios of 2:1, 1.5:1 and 1:1 were prepared by the incipient wetness impregnation method. The unmodified and modified chromium oxide catalysts were characterized for their surface area and by XRD, EPR and TPR techniques. No crystalline peak of or related to Cr_2O_3, and P_2O_5 were detected in the XRD of prepared samples. Clustered Cr^{3+}-O-Cr^{3+} species in addition to the γ-Cr^{5+}were detected by EPR. From the TPR studies, it was found that the reducibility (T_{max}) of the surface chromium species was not affected for the modified catalysts. The H/Cr molar ratio of the samples, however, decreased with phosphorus addition. The ODH of propane reaction studies revealed the effect of phosphorus on the propene selectivity and propene yield of the surface chromium oxide species. The conversion progressively decreased with phosphorus addition. Propene selectivity at iso-conversion increased till a chromium to phosphorus ratio of 1.5 and then decreased. Two power law (PL) models were considered to explain the reaction data. The power law model that considers a mechanism in which the propene is a primary product and the carbon oxides are secondary products is observed to be the best model to fit the reaction data. The kinetic parameters are obtained by minimization of an objective function using Genetic Algorithm. The pre-exponential factors decreased with phosphorus addition for most of the samples, however, the relative decrease was different. The activation energies and partial pressure exponents are not affected or affected randomly. Based on estimated kinetic-parameters the propene yield was calculated and observed to be maximum for the 1.5Cr1PTi catalyst. For this catalyst the ratio of the rate constant for propene degradation (k_2+k_3) to propane ODH (k_1) was the minimum.

Chapter-1

Introduction

Light alkenes are important building blocks in the modern petrochemical industry. They find application for the production of a wide variety of products. Consequently, the demand for alkene has been increasing. Due to this rising demand of alkenes, conversion of alkanes into their corresponding alkenes is an industrially significant process. Low cost of light alkanes and the fact that they are generally environmentally acceptable due to their low chemical reactivity have made them the ideal feedstock for alkene production. Accelerating global demand for alkene has spurred substantial interest in the development of alternative routes other than the traditional processes. Presently, steam cracking, catalytic cracking and dehydrogenation are mainly used as the direct route for the conversion of lighter alkanes to high value olefins.

The propene demand, mainly for production of polypropene, acrolein and acrylic acid, is increasing at a higher rate than the demand for ethylene and other light olefins co-produced in the traditional processes such as steam cracking and FCC of natural gas and oil fractions. Since the last few years, catalytic dehydrogenation of propane is also a topic of commercial as well as scientific interest as the better understanding of these reactions allows exploitation of cheap and abundant resources and selective production of propene. Despite the apparent simplicity of the reaction, however, the dehydrogenation processes possess several thermodynamic constraints, such as high endothermicity which require severe conditions of high temperature and low pressure [1]. Thermal cracking side reactions favored by high temperatures, significantly affect the stability of propylene and

alkenes produced. Thus, coke is deposited on all dehydrogenation catalysts, causing a drop in their activity [2, 3]. Consequently, frequent regeneration and complicated reactor designs are required. The thermodynamic and kinetic constraints have stimulated the search for better solutions.

To meet with all the above-sited challenges a potential new route, Oxidative Dehydrogenation (ODH), has been introduced for the production of alkenes [1, 4]. With the successful development of ODH, high olefin yields will be possible through the conversion of much smaller volumes of alkanes. Oxidative dehydrogenation (ODH) of alkanes is thermodynamically favored over a wide temperature range and offers the potential for the synthesis of alkenes with significant savings in energy and feedstock costs [1, 4–7].

Oxidative dehydrogenation (ODH) overcomes the thermodynamic limitations faced in the direct catalytic dehydrogenation process and the rapid coking of these dehydrogenation catalysts resulting in short catalyst life. In the ODH reaction, hydrogen is oxidized to water and there is no equilibrium limitation.

$$C_3H_8 + O_2 = C_3H_6 + H_2O \qquad \Delta H = -86 \text{ kJ/mol} \qquad (1.1)$$

This process has the potential to overcome the major technical problems associated with catalytic dehydrogenation. However, other problems arise that are related to the removal of the heat of reaction, control of selectivity due to the formation of undesired by-products and carbon oxides, the flammability of reaction mixture and the possibility of the run-away of the reaction. Selectivity to olefins remains a serious problem, as it limits the maximum achievable yield. Therefore, developing means of maximizing the alkene formation by minimizing side reactions is the major issue for the oxidative

dehydrogenation reactions. This can be achieved by the design of a catalyst that kinetically controls the oxidative dehydrogenation reactions to optimize the selectivity at higher conversions.

Recent studies have focused on using supported metal oxides for the ODH reactions due to their high degree of mechanical strength, better thermal stability and larger surface area [8, 9]. Previous studies dealing with supported metal oxide catalysts have shown that the nature of the surface metal oxide species depends on the oxide support, metal oxide loading, preparation method, and the presence of additives [10]. Of the various supported metal oxide systems supported chromium oxides are effective catalyst for ODH of propane [11-18]. They have been successfully used for dehydrogenation and other industrially important reactions [19-21]. Catalytic properties of the surface chromium oxide (chromia) species are observed to change due to the interaction between support and the chromium oxide species. It is also observed that the molecularly dispersed chromia species are more active for ODH of propane compared to bulk Cr_2O_3 [22]. It has been found that the specific activity of the surface chromium oxide species is highest for Cr_2O_3/TiO_2 compared to chromium oxide supported on other different supports (SiO_2, SiO_2-Al_2O_3 and Al_2O_3) [23]. However for Cr_2O_3/TiO_2 the propene selectivity was small. Therefore, it is essential to design a catalyst that optimizes both conversion and selectivity of ODH reaction.

Selective oxidation of hydrocarbons, of which ODH is a special case, requires redox and Lewis type acidic properties [24]. Furthermore, an acid-base bifunctional catalyst possessing weak acid- base pairs exhibits better catalyst activity and selectivity for the ODH reactions [25]. Thus, an ideal catalyst would require a proper combination of

redox and acid-base properties. Changes in the redox and acid-base properties can be brought about by using additives/modifiers. Such studies over Cr_2O_3/TiO_2 catalyst were performed by Cherian et al. [26]. Two types of additives were observed-interacting additives (Na) that co-ordinate with the surface chromia site and non-interacting additives (V, Mo) that co-ordinate with the titania support. Jibril et al. [27] studied alkali and molybdenum promoted Cr_2O_3/Al_2O_3 catalyst and noted that a particular composition of cesium-molybdenum-chromium on Al_2O_3 exhibited a propane conversion of 15.1% and a propene selectivity of 64.5%. For the ethane ODH reaction phosphorus was used as a promoter for the Cr_2O_3/TiO_2 catalyst and an optimum Cr:P ratio was required to optimize yields. A few other studies exist that study the effect of promoters on supported chromium oxide catalyst [28, 29].

The above studies do not, however, provide details on the effect of promoters on the reaction mechanism of alkane ODH. Knowledge of the ODH mechanism is essential to understand the functioning of the catalyst and devise methods to improve it. One of the methods to improve the knowledge of the alkane ODH mechanism is by analysis of the reaction kinetics with the help of kinetic-parameters. Although several metal oxide based catalytic systems have been studied for the ODH reactions, only a few studies are aimed at understanding the mechanism especially by analysis of the kinetic-parameters. Moreover, no significant studies are reported on the kinetics, reaction mechanism and kinetic-parameters of ODH reaction over any modified supported chromium oxide catalysts to explain the effect of the modifier.

Determination of kinetic-parameters for a particular reaction mechanism is not a straightforward task. It requires proper design, modeling and data collection for the

reactor. Furthermore, determination of the kinetic-parameters requires solution of ordinary differential equating initial value problems such that differences between observed and predicted concentrations are minimized. Several optimization techniques have been used to obtain the kinetic-parameters. Recently, the application of genetic algorithms (GAs) as an optimization tool for kinetic-parameter estimation has gained importance since global optima are achieved and initial guesses of parameters are not required.

1.1 Objective of study

The objective of the present study is to understand the effect of modifiers on Cr_2O_3/TiO_2 for the ODH of propane. Phosphorus was chosen as a modifier since higher yields are achieved. A 3wt. % Cr_2O_3/TiO_2 catalyst is chosen as the base catalyst to understand the effect of phosphorus modification on the propane ODH reaction. The 3% Cr_2O_3/TiO_2 was chosen since only surface active chromium oxide species are present [26]. To achieve the objective, a series of catalysts are synthesized by loading titanium dioxide (TiO_2) with chromium oxide and different amounts of phosphorus. The synthesized catalysts are initially characterized through various characterization techniques like BET, X-ray diffraction, electron paramagnetic resonance and temperature programmed reduction to examine the possible structural changes on the catalyst surface. The unmodified and modified Cr_2O_3/TiO_2 catalysts are then studied for the ODH of propane at different operating conditions to understand the effect of phosphorus modification. The kinetic-parameters are estimated using a genetic algorithm and related to the structural changes.

Finally, the effect of phosphorus modification is proposed by obtaining the structure-reactivity relationship.

1.2 Thesis organization

The thesis contains five chapters of which the current chapter is the first. The next chapter, Chapter two, presents a brief literature review related to the present study. In Chapter three, details regarding preparation of the catalyst, characterization techniques, experimental set-up and the methodology for kinetic-parameter estimation are provided. The results obtained from the characterization and reaction studies of unmodified and modified Cr_2O_3/TiO_2 catalysts on the ODH of propane are presented and discussed in Chapter four. Conclusions and recommendations for future work are reported in Chapter five. In each chapter the Tables and Figures are given at the end in numerical order. The references used throughout the thesis are given at the end in numerical order as they appear in the text. Finally, the raw data for propane ODH over the catalysts are given in the Appendix.

Chapter-2

Literature Review

Supported chromium oxide catalysts have been successfully used for the ODH of alkanes [20, 30, 31]. Unfortunately, alkene selectivity obtained by this catalyst system is very low. Bras et al. [24] observed the requirement of redox and Lewis acidity properties in the catalyst for the selective oxidation of hydrocarbons to corresponding alkenes. It has also been proposed that an acid-base bifunctional catalyst possessing weak acid- base pairs would exhibit better catalyst activity and selectivity for the ODH reactions [25]. Previous studies suggest that the introduction of an additive or modifier to the unsupported metal oxide catalysts is useful for better alkene selectivity [32-37]. Till date, however, very few studies exist that discuss the effect of modifiers for supported chromium oxide catalysts. A brief literature review of the influence of additives on the structure-reactivity relationship of supported metal oxides, in general, and supported chromium oxide, in particular, for the ODH of alkane is given below. This literature review also gives a brief detail about Genetic Algorithm (GA), which is used as an optimization tool for finding out the kinetic parameters involved with the reactions.

Ziyad *et al.* [38] studied the effect of phosphorus additive on Cr_2O_3/TiO_2 catalyst for ODH of C_2H_4 and observed that the presence of chromium oxide notably increases the activity toward the total oxidation of hydrocarbon. The addition of phosphorus to the system improved the global conversion and the ethylene selectivity. An optimum P/Cr value at which the conversion and selectivity are best was reported. Characterization of the catalysts was achieved by XRD, EPR and UV-visible

spectroscopy. XRD patterns revealed that the TiO_2 did not suffer any structural modification after impregnation. EPR and UV- visible spectroscopies revealed that the sample essentially contained Cr^{6+} and Cr^{5+} ions, which were not very efficient in mild oxidation. They concluded that the improvements in catalytic activity and selectivity, due to addition of phosphorus, can be attributed to the appearance in the samples of phosphates and clustered Cr^{3+} ion.

Osiysky et al. [39] studied the chromium phosphate catalyst for the oxidation of n-C_2H_4. The kinetic regularities of the n-C_4H_{10} catalytic transformation into $CrPO_4$ have been investigated. The kinetic parameters of the n-butane oxidation reaction and the catalytic transformation schemes were suggested. The product maximum output condition under a partial n-butane oxidation on the chromium phosphate catalyst was suggested.

Maiti et al. [40] investigated the effect of surface phosphorus on the oxidative dehydrogenation of C_2H_6 and found out that a phosphorus-enriched surface enhances the ODH yield of ethane to ethylene. To understand the role of phosphorus, they carried out the ODH reactions on a silica surface, with and without phosphorus, using the density functional theory code DMol3 in a periodic super-cell. The simulation study revealed that activation barriers for the rate-limiting steps are lowered by 10 kcal/mol in the presence of phosphorus. This decrease results from a transition state in which the phosphorus atom remains quasi-5-valent and fourfold coordinated.

Sidorchuk et al. [41] determined the effect of different metal phosphates on the partial oxidation of C_4H_{10} by comparing the catalytic activities of Al, Cr, Fe, Ti, Zr, Sn, and V phosphates. It was observed that except for V phosphates, the products were

mainly CO and CO_2. The $(VO)_2P_2O_7$ phase exhibits maximum activity and selectivity for maleic anhydride formation.

Loukh et al. [42] studied the oxidative dehydrogenation of C_2H_6 to C_2H_4 on V- and Cr-based phosphate catalysts at 550°C. Vanadium and chromium cations were introduced in zirconium hydrogen phosphates either by cationic exchange of their acidic proton or by impregnation with VO^{2+} and Cr^{3+} and then compared to $(VO)_2P_2O_7$ and $CrPO_4$ pure phases. They reported that VO^{2+} and Cr^{3+} on the $\alpha Zr(HPO_4)_2.2H_2O$ phase were more selective toward ethylene. The $(VO)_2P_2O_7$ and to a lesser extent $CrPO_4$ were even more selective toward C_2H_4 at similar conversion levels. UV, ESR, XRD, IR, and SEM were used for the characterization of the catalysts after catalytic testing at 823K. Based on the obtained data they concluded that the catalytic features were related to V and Cr local arrangements (small clusters or chain arrangements) and to the counter anion, O^{2-} or PO_4^{3-}. The best catalyst for ethane oxidative dehydrogenation consisted of VO^{2+} and Cr^{3+} chains separated. by PO_4^{3-} anions.

Huff and Flick [14] examined the ODH of C_2H_6 using Cr_2O_3 and Pt-modified Cr_2O_3 -coated ceramic foam monoliths and Cr_2O_3/Al_2O_3 pellet catalysts. They observed the high C_2H_4 selectivity and C_2H_6 conversion over the Cr_2O_3 catalysts compared to Pt-coated monoliths. The 10 wt.% Cr_2O_3/ZrO_2 monolith catalyst produced the best results of all catalysts examined, giving C_2H_4 selectivities of 70% at a C_2H_6 conversion of about 80% compared to a C_2H_4 selectivity of 65% at a C_2H_6 conversion of 75% under the same conditions over the Pt/α-Al_2O_3 monolith catalyst.

Ramis and Busca [43] reported the effect of several modifiers on supported chromium oxide catalysts. For example when an alkaline earth metal was added, the

lewis acidity decreased whereas non-metallic dopant ($SO4^{2-}$, PO^{4-}) increased the lewis acidity. Elements such as Mo^{4+}, W^{4+}, V^{4+} etc. which are non-interactive will not affect the structural of surface chromyl species, however, will be competitive with the basic sites of the support in the reaction. The effect of additives on the reactivity of each supported catalysts will be unique as their influence on the activity depends upon the reaction mechanism.

Neri et al. [44] investigated the oxidative dehydrogenation (ODH) of iso-C_4H_{10} on Ca-doped chromium oxide catalysts supported on Al_2O_3. They observed dispersed Cr^{3+} and Cr^{6+} species in addition to Cr_2O_3 and $CaCrO_4$ crystallites on the alumina surface. The relative amount of the chromium species depends on the Ca loading. The Cr^{3+}/Cr^{6+} ratio decreases on increasing the Ca loading due to the preferred formation of bulk chromate species. The Ca loading affects the reducibility of the Cr^{6+} species and the acid sites strength distribution of the catalysts.

Grzybowska et al. [11] performed ODH of iso-C_4H_{10} on chromia supported on SiO_2, Al_2O_3, TiO_2, ZrO_2, and MgO. They also examined the effect of potassium-modification. The supported catalysts have found to be active in the ODH of isobutene at relatively low temperatures 200-400°C and the total activity and selectivity to isobutene is dependent on the nature of the support and the potassium presence. The highest selectivity to isobutene (70% at 5% conversion) and the isobutene yields of 9% were obtained for CrO_x/ TiO_2 and K- promoted CrO_x/Al_2O_3 catalysts.

2.1 Kinetic Modeling of ODH

In the last few years several studies were made on the structure and reactivity of ODH of propane over supported chromia and vanadia catalysts. However, only a few kinetics and

mechanistic studies on the oxidative dehydrogenation of propane over supported metal oxides are reported. A brief literature survey on the kinetic study for ODH and kinetic parameter estimation is given below.

2.2 Kinetic Study for ODH

Kinetic isotopic studies were carried out with supported V_2O_5 catalysts assuming a first order dependency with partial pressure of propane [45]. It was observed that CO_2 is formed by primary decomposition of propane and secondary decomposition of propene, whereas CO is formed by the secondary decomposition of propene. A Mars-Van Krevelen redox mechanism involving two lattice oxygens in irreversible C-H bond activation was proposed. In these reaction mechanisms, the reaction rates were proposed to be independent of oxygen partial pressures. Chen et al. [46] suggested that the lattice oxygen in the primary dehydrogenation and combustion were different. Chen et al. [47] investigated ODH of propane over supported V, Mo and W oxides and concluded that the mechanism was the same for all these catalysts. It was suggested that the propane ODH and propene combustion rates depends upon the C-H bond energy difference and also on the adsorption enthalpies of propene and propane.

Creaser [48] studied the partial pressure dependencies of propane oxidation. The corresponding rate expression, which is in accordance with Rideal type rate expression for various concentrations of vanadium on amorphous $AlPO_4$, is adequate to explain the partial pressure dependencies of both oxygen and propane. A first order dependency of propane for the ODH reaction is proposed.

Creaser and Andersson [49] have undertaken a detailed kinetic investigation of ODH on V-Mg-O catalyst. Various rate expressions are derived in order to fit the data based on Power Law type models and mechanistic models, such as, Langmuir-Hinshelwood and Mars-Van-Krevelen models. In these models, carbon oxides were considered as secondary products.

Grabowski et al. [50] tested various kinetic models on the propane oxidative dehydrogenation on the V_2O_5/TiO_2 catalyst. Numerical methods (the Runge–Kutta method combined with the Levenberg–Marquardt method) were applied to solve the systems of differential equations describing the kinetic of the ODH. It was observed that the steady-state model, in which the surface oxygen plays an important role, provided the best description of the experimental results. The analysis of the reaction network indicated that propene is the only useful product primary produced, and that CO and CO_2 are produced largely by the sequential oxidation of the in situ produced propene, and to a lesser extent by a parallel route of the direct deep oxidation of propane.

Bottino et al. [51] studied the kinetic of propane ODH on a V/γ-Al2O3 catalyst prepared by the adsorption technique. The kinetic parameters were determined through non-linear regression analysis. Two approaches were applied. In the first one, power law expressions were used to describe the network of reactions involving propane, propylene, CO and CO_2. In the second approach, the experimental data was fitted with a rate equation obtained by assuming that molecular oxygen re-oxidizes the active site reduced by the surface.

Parameter estimation using traditional methods, such as, Levenberg-Marquardt's method depend strongly on initial guesses values. On the other hand, objective functions

based on non-linear models are common features in most recent parameter estimation problems. These nonlinear models generally contain more than one minimum, consequently, requires a tedious algorithm, which sometime reaches to non-global optima. Thus, there is a need for development of efficient algorithms to replace the traditional methods. One such class of algorithms known as Genetic Algorithms (GA) fulfils this need satisfactorily and shows promising results in terms of its accuracy and efficiency.

2.3 Kinetic Parameter Estimation

Conventionally, nonlinear regression method has been used for obtaining kinetic parameters but its use for a case of multi-response and correlated systems is not an appropriate one [52]. It is proposed that a determinant criterion can be considered to be the best one for obtaining the kinetic parameters for the above mentioned case. Genetic algorithm has recently replaced the nonlinear regression methods to optimize the determinant. Genetic algorithm (GA) is used to find approximate solutions to difficult-to-solve problems.

In an attempt to find initial estimates of rate constants for non-linear chemical kinetics, Wolf *et al.* [53] have exploited GA techniques without a priori assumptions of rate determining step in order to apply for the wide range of partial pressures of reactants and temperatures. Elliot *et al.* [54] have used inversion procedure of genetic algorithm to estimate rate parameters corresponding to product species measurement data from combustion of fuel experiments. This study suggests that its wide application to other chemical kinetics and optimization of other higher order kinetics is possible. Polifke *et al.* [55] employed genetic algorithm to investigate the kinetic parameters of simplified

reaction mechanism for methane combustion. It is also determined that using genetic algorithm requires minimum human effort and little insight into the details of chemical mechanism to generate reliable kinetic parameter.

Several of studies have been made to implement GA for obtaining kinetic parameters. The performance of genetic algorithm strongly depends on the genetic algorithm running parameters. Furthermore, it is observed that the application of genetic algorithm to generate a good initial point for the non-linear local convergence method requires less computing time and increase the reliability of the parameters.

2.4 Genetic algorithm (GA)

GA algorithms mimic evolution and natural selection to solve a problem [56-58]. Due to this the stronger individuals are likely to be the winners in a competing environment. GA's are gaining immense popularity for their potential as an optimization technique that can effectively search in the bounds of the complex problems. These are multidirectional search and optimization procedures that combine survival of the fittest among a set of string structures with structured yet randomized information. Optimal binary strings are located by processing an initially random population of strings using artificial mutation, crossover and selection operators, in an analogy with the process of natural selection. In this way better models or solutions can be bred from an originally random starting population.

Initially a population of individuals (solutions) is created, each represented by a chromosome (a collection of genes or characteristics) to form an initial pool of possible solutions for the given objective function to be optimized. This is called the first

generation pool. All of the chromosomes, having a particular fitness value, are evaluated by an *objective function* and effectively the pool is sorted with those having better fitness at the top, representing better solutions to the problem.

The next step of the algorithm is to generate a second generation pool of parameter lists, which is done using the genetic operator, selection, crossover and mutation.

- **Selection:** The first step in the construction of the next generation is to *select* a pair of chromosomes for crossover by some well-defined selection methods like *roulette wheel selection, tournament selection* etc. Tournament selection is used in the present study. Selection is more biased towards elements of the initial generation which have better fitness value. This process is repeated until the new offspring pool is full.

- **Crossover:** Following selection, the *crossover* (or *recombination*) operation is performed upon the selected chromosomes. In general, two parent chromosomes are chosen to reproduce and their crossover results in two new child chromosomes, which are added to the second generation pool. This is repeated until there are an appropriate number of candidate solutions in the second generation pool.

- **Mutation:** The next step is to mutate the newly developed pool, again by a process of selection, this time of individual chromosomes, followed by application of the *mutation* genetic operator. The main role of mutation is to provide genes not present in the initial population so as to prevent stagnation at local optima.

These processes result in a second generation pool of chromosomes that is different from the initial generation, which is then evaluated and the fitness values for each list is obtained. Generally the average degree of fitness will have increased by this procedure for the second generation pool. The process continues by generating third, fourth, fifth and future generations, until one of the generations contains solutions which are acceptable.

A flowchart explaining all the major operations of GA as briefly discussed above is shown in Fig. 2.1.

2.5 Summary

Thus, previous studies suggest that better selectivity and reactivity performance of supported chromium oxide and other metal oxides modified with additives like P, K, Ca, La is possible. Furthermore, phosphorus improves the activity and selectivity of the catalysts in the ODH of alkanes by introducing some specific redox and acid-base properties in the supported compound. In the present study, to understand the effect of phosphorus as a modifier, a P-Cr_2O_3/TiO_2 with different chromium to phosphorus molar ratios are synthesized and then its effect on the structure and reactivity behavior of the catalysts is studied. By estimating the kinetic parameters also, an understanding of the role of phosphorus as a modifier, for the ODH of propane, is developed.

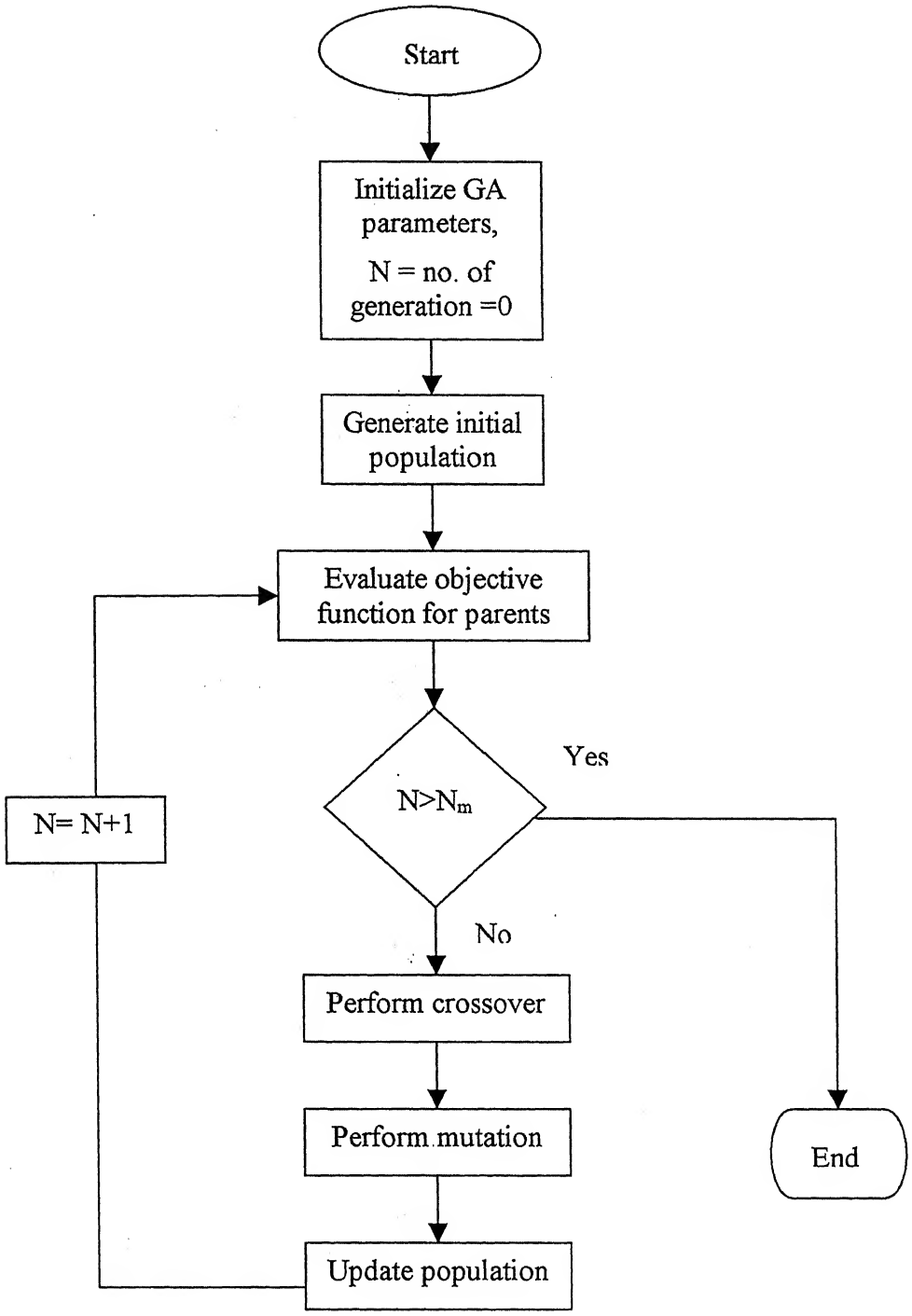

Figure 2.1 A flowchart of the working principle of GA

Chapter-3

Experimental Details

3.1 Sample Preparation

The incipient wetness impregnation method was employed to synthesize the titania supported unmodified and modified chromium oxide catalyst samples. This method is known for its simplicity and viability for making low amounts of metal oxide catalysts [59]. Modified catalysts were prepared by co-precipitation of chromium and phosphorus ions. Titania (TiO_2, Degussa, P-25) was used as a support. Chromium nitrate nonahydrate ($Cr(NO_3)_3.9H_2O$, Aldrich, 99.98% purity) and diammonium hydrogen ortho-phosphate ($(NH_4)_2HPO_4$, S. D. Fine-Chem Ltd.) were used as the precursors for the chromium and phosphorus, respectively. Initially, the titania support was pretreated with incipient volumes of double distilled water. The support was then dried at room temperature in a desiccator followed by drying at 383 K for 8 h. Finally, the support was calcined at 723 K for another 8 h.

The incipient wetness volume of solution was prepared by adding precalculated amount of chromium nitrate nonahydrate and diammonium hydrogen ortho-phosphate to double distilled water. The mixture containing chromium precursor, phosphorous precursor and water was stirred until a homogeneous solution was formed. For preparing the unmodified chromia-titania (CrTi) catalyst the phosphorus precursor was not required, and similarly, for the phosphorus-titania (PTi) catalyst the chromium precursor was not required. The above solution containing chromium and/or phosphorus ions was

intimately mixed with the pretreated support to form a paste. The paste was dried at room temperature for 12 h, followed by drying at 383 K for 12 h and finally calcined at 723 K for 12 h.

In the present study five catalyst samples were prepared. The nomenclature of the CrTi and PTi samples were based on the weight percent of the Cr_2O_3 and P_2O_5 present in the sample. The nomenclature of the modified CrTi catalysts was based on the molar ratio of chromium to phosphorous on the TiO_2 support. The nomenclature and composition of the samples synthesized are tabulated in Table 3.1.

3.2 Characterization

3.2.1. Surface Area Studies

The surface areas of the samples were obtained using the multi-point BET method. A bench-top **COULTER SA 3100** analyzer equipped with **SA-VIEW TM** software using N_2 adsorption at 77K was used for this purpose.

3.2.2. X-Ray Diffraction (XRD) Studies

X-Ray diffraction patterns were obtained in the range of 20-80^0(scanning rate: 10 ^{0} min^{-1}) with a 180 Debye flex-2002 X -ray powder diffractometer equipped with a monochromator. Ni filtered K_α radiation from a Cu target (λ= 1.54056 A°) was used.

3.2.3. Temperature Programmed Reduction (TPR) Studies

The TPR studies were carried out in a microreactor containing 0.035g of the sample and attached to a Micromeritus Pulse Chemisorb 2705 analyser. The same amount of each sample was used for the TPR studies. Helium was used as a carrier gas and also to degas

the samples prior to the reduction experiments. The carrier gas flow was adjusted to a fixed value between 30 and 50 cc/min. Degassing of the sample was achieved at 523 K for 0.5 h. A 5% H_2/Ar mixture flowing at 40 sccm was used for reduction and the temperature was ramped at a rate of 10 K/min from ~ 373 to 973 K. The amount of hydrogen consumed was detected using a TCD.

3.2.4. Electron Paramagnetic Resonance (EPR) Studies

The EPR spectra were obtained in a BRUKER EMX 1444 EPR spectrometer. The spectra were obtained under ambient conditions using a microwave frequency of ~ 9.86 GHz and a microwave power 0.20 mW. The scan time was 8 min and the magnetic field modulation frequency was 100 kHz. The microwave radiation travels down a waveguide (a type of rf pipe) to the sample, which is held in place in a microwave 'cavity' positioned between the poles of two magnets. Spectra are obtained by measuring the absorption of the microwave radiation while scanning the magnetic-field strength. The EPR spectra are displayed in derivative form to improve the signal-to-noise ratio and were calibrated with DPPH using a duel cell.

3.3 Reactivity

3.3.1 Experimental Set-up

The ODH of propane (C_3H_6) is performed in a fixed bed, down-flow, tubular quartz reactor. The reactor was a single piece of quartz with an inlet of 10 mm inner diameter and an outlet of 5mm outer diameter. Schematic of the reaction set-up is shown in Fig. 3.1.

As shown in Fig. 3.1 two separate thermal Mass flow Controllers (**Bronkhost Hi-Tech, Model F-201D and Model F-201C)** were used to individually control the flow rate of propane and air. The two gases are mixed at a T-junction and then sent to the reactor. The reactor tube was mounted vertically in a tubular furnace. The catalyst bed containing the catalyst and quartz powder mixture was placed on quartz wool at the center of the 300 mm long quartz reactor. Quartz powder acts as a diluent with the catalyst to prevent temperature gradients and to avoid the channeling of gas within the catalyst bed. A chromel-alumel thermocouple was inserted from the top of the reactor to measure the temperature of the reactor and the catalyst bed. It was placed in such a manner that the tip of the thermocouple remains just above the catalyst bed. The temperature of the catalyst bed was controlled by a PID temperature controller (**FUJI Micro-Controller X Model PXZ-4).**

Product gases were analyzed using an online gas chromatograph (**AIMIL NUCON 5765**) using a Hysep-Q column for separation of hydrocarbons, CO and CO_2. Reaction products were detected with the help of a Flame Ionization Detector (**FID**). Propene (C_3H_6), CO and CO_2 were found to be the main reaction products. A methanizer attached with gas chromatograph converts the carbon oxides (CO and CO_2) to methane in order to be detected by the FID. No oxygenated products were found. Several runs were taken at each experimental condition to ensure that steady state conditions was achieved.

Blank experiments were also performed to determine the homogeneous contribution to the reaction. The fact that no reactions occurred in the blank experiments indicated that gas-phase-initiated reactions did not occur at the reaction conditions considered. In addition, reactions in the gas phase involving desorbed radical species

were not considered to play a role due to the moderate reaction temperatures and precautions taken to minimize the void gas volume in the reactor.

3.3.2 Reaction Studies

Two types of reaction studies were considered:

i. Contact time variation studies

ii. Operating conditions variation studies.

3.3.2.1 Contact time variation studies

Contact time studies for ODH of propane were performed using 0.2g of 3% Cr_2O_3/TiO_2 and phosphorus modified CrTi catalyst samples at 2:1 C_3H_8:O_2 ratio with a total flow rate ranging from 20 to 120 cc/min. Temperature was kept constant at 653 K for all the catalysts. For each operating condition two runs were taken and average was reported.

The effect of contact time, W/F_{A0}, on the conversion and selectivity was studied where W is the weight of the catalyst and F_{A0} is the total flow rate.

3.3.2.2 Operating conditions variation studies

The operating conditions considered were C_3H_8:O_2 molar ratio and temperature. A physical mixture of 0.2 g of the catalysts and required amount of quartz glass powder to form a bed height of 1 cm was used for this reaction study. Experimental runs were performed at three different temperatures of 633, 653 and 673 K with a constant total flow rate of 75 cc/min. The C_3H_8:O_2 flow ratios were varied from 1:1 to 3:1.

3.3.2.3 Analysis of reaction data

The products analyzed from the reaction outlet were C_3H_6, CO, CO_2 and unconverted C_3H_8. Each of these components gave separate areas in the chromatograph, which were then converted to mole fractions based on their response factor. The mole fractions were then used to calculate the conversion, selectivity and yield per gram catalyst as per the formula given below.

i. Conversion

Conversion for the reaction was calculated by using the following formula,

$$\text{Propane Conversion (\%)} = (n_c / n_f) \times 100 \quad (3.1)$$

ii. Selectivity

Product selectivity for the reaction was calculated by using the following formula,

$$\text{Product Selectivity (\%)} = (n_{hc} / n_c) \times (N_{hc} / N_P) \times 100 \quad (3.2)$$

iii. Propene Yield

The amount of propene formed based on the inlet propane was represented by yield, which was calculated as follows:

$$\text{Propene yield (\%)} = (n_{hc} / n_f) \times (N_{hc} / N_P) \times 100 \quad (3.3)$$

iv. Carbon Balance

Carbon balance represents the accuracy of measurements and it provides an indicator as to whether carbon is deposited on the catalyst. Carbon balance calculations are done based on the following formula,

$$\text{Carbon balance} = (N_{hc} / N_P) \quad (3.4)$$

Where,

n_c number of moles of propane consumed

n_f number of moles of propane fed

n_{hc} number of moles of products formed. The products formed are propene, CO and CO_2

N_{hc} the number of carbon atoms present in the products

N_p the number of carbon atoms present in the propane

3.3.3 Modeling of the Reactor and Kinetic Parameter Estimation

Modeling of the reactor is achieved by the integral method. With appropriate reactor modeling the kinetic-parameters are estimated for steady state reactor operation.

3.3.3.1 Modeling of the reactor and problem formulation

To model the reactor the following assumption were made.

- The reactor operates under isothermal and steady state condition
- Total number of moles of gases remain constant
- There is no heat and mass transfer limitations
- Gas phase reactions are negligible
- Catalyst activity remains constant. (Negligible catalyst deactivation)

All assumptions are justified since propane conversions are low and feed gases are diluted with nitrogen.

The differential material balance equation for each component, i, for a particular reaction network can be written as

$$V_0 y_i \mid_W - V_0 y_i \mid_{W+dW} - \sum_j n_{ij} r_j dW = 0 \qquad i = 1.....v \tag{3.5}$$

Where,

V_0 = volumetric flow rate of the feed, m^3/s

y_i = mole fraction of the i^{th} component

n_{ij} = stoichiometric coefficient of the i^{th} component for the j^{th} reaction

r_j = rate of j^{th} reaction and is a function of K_j or $r_j = f_j(y_i, K_j)$

K_j = kinetic parameters for the j^{th} reaction

v = number of components

W = weight of the catalyst, kg.

The above equation with the assumptions mentioned can be simplified and written as follows,

$$\frac{dy_i}{dW} = \sum_j n_{ij} r_j \Big/ V_0 \tag{3.6}$$

Equation (3.6) is a set of ordinary differential equations initial value problems (ODE-IVPs). The set of ordinary differential equations represented by Eqn. (3.6) can be simultaneously solved to obtain the output mole fraction of each component based on the input initial value of mole fraction of each component, y_{io}, and temperature, provided the weight, stoichiometric number, n_{ij}, volumetric flow rate, V_0, the function dependence $r_j = f_j(y_i, K_j)$ and kinetic parameters are known. The input mole fraction is changed during integration over the entire mass using Runga-Kutta fourth order technique to give the output mole fraction.

The rate of reaction, r_j, is a function of kinetic-parameter, K_j. For a particular set of input kinetic-parameters, the output mole fraction can be determined by integrating the above equation. Thus, comparison of the actual output mole fraction, $y_{i,expt}$, with those

predicted by assuming certain values of K_j, $y_{i,predicted}$, can be used as a basis to calculate K_j. Since the kinetic-parameters have Arrhenius dependence on temperature non-linear regression analysis is required to obtain rate constants.

The response data, the output mole fraction of C_3H_8, C_3H_6, CO and CO_2, are assumed to be well described by a nonlinear model given by

$$Y_h = g_h(\theta, y) + Z_h, \qquad h = 1, 2, \ldots, v \tag{3.7}$$

where,

Y_h = vector of random variables representing the response variable

Z_h = error associated while calculating the response h

θ = parameter vector

y = concentration vector

$g_h(\theta, y)$ = predicted concentration

The predicted output mole fraction of the i^{th} component in the u^{th} experiment, $y_{iu,pred}$ obtained this way can then be compared with the actual output mole fraction $y_{iu,actual}$. An objective function involving the predicted and actual mole fractions of the components is minimized to obtain the best value of the kinetic parameters.

For multiresponse systems and when responses are correlated, the ideal criterion is the minimization of the following determinant [60-63].

$$\det \begin{vmatrix} \Sigma (y_{1u} - y_{1u,\,pred})^2 & \Sigma [(y_{1u} - y_{1u,pred})(y_{2u} - y_{2u,pred})] & \Sigma [(y_{1u} - y_{1u,pred})(y_{3u} - y_{3u,pred})] & \Sigma [(y_{1u} - y_{1u,pred})(y_{4u} - y_{4u,pred})] \\ \Sigma [(y_{1u} - y_{1u,pred})(y_{2u} - y_{2u,pred})] & \Sigma (y_{2u} - y_{2u,pred})^2 & \Sigma [(y_{2u} - y_{2u,pred})(y_{3u} - y_{3u,pred})] & \Sigma [(y_{2u} - y_{2u,pred})(y_{4u} - y_{4u,pred})] \\ \Sigma [(y_{1u} - y_{1u,pred})(y_{3u} - y_{3u,pred})] & \Sigma [(y_{2u} - y_{2u,pred})(y_{3u} - y_{3u,pred})] & \Sigma [(y_{3u} - y_{3u,pred})^2 & \Sigma [(y_{3u} - y_{3u,pred})(y_{4u} - y_{4u,pred})] \\ \Sigma [(y_{1u} - y_{1u,pred})(y_{4u} - y_{4u,pred})] & \Sigma [(y_{2u} - y_{2u,pred})(y_{4u} - y_{4u,pred})] & \Sigma [(y_{3u} - y_{3u,pred})(y_{4u} - y_{4u,pred})] & \Sigma [(y_{4u} - y_{4u,pred})^2 \end{vmatrix} \quad (3.8)$$

The problem then can be formulated as minimization of the above determinant. Minimization of the determinant is achieved by applying Genetic Algorithm.

3.3.3.2 GA – Optimization Technique

The optimization technique applied in the present study is a Genetic Algorithm (GA). It is considered to be robust and efficient method for optimization. The performance of genetic algorithm strongly depends on the genetic algorithm running parameters as discussed in Chapter-2. Here a brief detail of source code and the GA parameters used in the present study to estimate the kinetic-parameters is given.

3.3.3.2.1 Source Code

A NSGA code (Non-dominated Sorting Genetic Algorithm) has been used in the present study to determine the kinetic parameters. The NSGA code is taken from the KANGAL lab of IIT Kanpur, and has been developed by Deb and co-workers.

The GA implementation is restricted to real coded variables only. All constraints are greater-than-equal-to type (g >= 0) and normalized. Evaluation is done based on the determinant criterion. The above determinant is coded and the best values of the kinetic parameters are estimated by minimization of it.

3.3.3.2.2. GA Parameters

Initially a population of solution is randomly generated. The size of population was chosen in between 120 and 200 for power law type models. The variable boundaries are fixed for each parameter and fixation of boundaries is done according to previous knowledge of the parameters. Selection of parents from the pool of solutions is done by tournament selection. The size of tournament in the present study was 2. Crossover probability exchanges information among parent solutions, whereas polynomial mutation operator is utilized to introduce the extra diversity to the solutions. The values of crossover and mutation probability were 0.8-0.9 and 0.1-0.2, respectively. Simulated binary crossover operator (SBX) is used. In this real coded GA that chases the function optima wherever it goes in the search space. The exponents of SBX and mutation were 2 and 200 respectively. The termination criteria used in this GA code was the number of generation. Number of generations was varied from 1,000 to a maximum of 30,000.

3.4 Reaction Models

The kinetic study of propane ODH involves various proposed reaction models. These proposed models can be broadly classified as Power law type and mechanistic type. According to these models propene is a primary product of propane. However, the formation of carbon oxides as primary, secondary or tertiary products is still debatable. Here discussion is confined to Power Law based models and details about mechanistic models, such as Langmuir-Hinshelwood model, Rideal type model and Mars-van-Krevelen model are not considered.

3.5 Reaction Scheme

The generalized reaction network for the ODH of propane is shown in Fig.3.2. Here the reaction of the carbon containing molecules with oxygen is presented in the form of six reaction steps, r_1 to r_6. Propene is formed by the ODH of propane (r_1). Propene can degrade to form CO and CO_2 by reactions r_2 and r_3, respectively. The carbon oxides, CO and CO_2, can also be formed directly from propane by reactions r_4 and r_5, respectively. Finally, CO_2 can also be formed by the oxidation of CO by reaction r_6.

The stoichiometric equations corresponding to each reaction step in the reaction network is given by equations (3.9) to (3.14).

$$C_3H_8 + 0.5O_2 \rightarrow C_3H_6 + H_2 \quad (3.9)$$

$$C_3H_6 + 3O_2 \rightarrow 3CO + 3H_2O \quad (3.10)$$

$$C_3H_6 + 4.5O_2 \rightarrow 3CO_2 + 3H_2O \quad (3.11)$$

$$C_3H_8 + 5O_2 \rightarrow 3CO_2 + 4H_2O \quad (3.12)$$

$$C_3H_8 + 3.5\,O_2 \rightarrow 3CO + 4H_2O \quad (3.13)$$

$$CO + 0.5O_2 \rightarrow CO_2 \quad (3.14)$$

3.6 Power Law Models

In the power law models it is assumed that the reaction rate is proportional to the partial pressure of reactant raised to a particular exponent. Based on the reaction steps given by Eqns. 3.9 to 3.14 the reaction rates are given by Eqns. 3.15 to 3.20.

$$r_1 = k_1 (P_{C_3H_8})^{a_1} (P_{O_2})^{b_1} \quad (3.15)$$

$$r_2 = k_2 (P_{C_3H_6})^{a_2} (P_{O_2})^{b_2} \quad (3.16)$$

$$r_3 = k_3 (P_{C_3H_6})^{a_3} (P_{O_2})^{b_3} \quad (3.17)$$

$$r_4 = k_4 (P_{C_3H_8})^{a_4} (P_{O_2})^{b_4} \quad (3.18)$$

$$r_5 = k_5 (P_{C_3H_8})^{a_5} (P_{O_2})^{b_5} \quad (3.19)$$

$$r_6 = k_6 (P_{CO})^{a_6} (P_{O_2})^{b_6} \quad (3.20)$$

Where,

k_i is the i_t^h rate constant for reaction i and is a function of the pre-exponential factor, k_{io}, and activation energy, E_i

a_i and b_i are the partial pressure exponent of the reactants for reaction i.

Thus, each reaction, r_i, involves four parameters: k_{io}, E_i, a_i and b_i.

Based on previous studies only two power law models were analyzed to determine the empirical reaction rates. These two power law models PL-1 and PL-2 are described below.

3.6.1. PL-1 Model

The PL-1 model assumes that CO and CO_2 are secondary products formed from propene. Thus, r_1, r_2 and r_3 are the only reaction steps considered. There are 12 parameters in this consecutive reaction model; four for each reaction step. This type of reaction scheme has been considered previously [49]. A schematic of the PL-1 model is given in Fig. 3.3.

3.6.2. PL-2 Model

The PL-2 model takes into consideration r_1, r_4 and r_5 reactions. Thus, C_3H_8 reacts with oxygen and produces C_3H_6, CO and CO_2 from r_1, r_4 and r_5, respectively. Consequently, C_3H_6, CO and CO_2 are primary products. There are 12 parameters also in the PL-2 model. A schematic of the PL-2 model is given in Fig. 3.4. The parameters involved in the PL-1 and PL-2 models are given in Table 3.2.

3.6.3. Reparameterisation of reaction rates

Parameter estimates obtained by fitting models to data are often highly correlated with each other. Under such circumstances the parameters are of little use for predicting the nature of the system. In chemical kinetics high correlations are frequently encountered between estimates of the kinetic-parameters in the Arrhenius expression for a rate constant making the analysis of a reaction network very difficult [64]. For both models considered here the reparameterized rate constants are expressed in Arrhenius form as

$$k_i = k_{i\,o} \exp[\frac{-E_i}{R}(\frac{1}{T} - \frac{1}{T_m})] \tag{3.21}$$

Where,

k_{i0} = pre-exponential factor

E_i =activation energy for the reaction i, kJ/mol

R = universal gas constant, kJ/kmol K

T = actual reaction temperature, K

T_m = mean temperature, K

The inverse temperature is centered about the inverse mean temperature ($1/T_m$). Furthermore, the partial pressure of a component, P_j, is also centered about the mean partial pressure of the component, i.e., $(\frac{P_j}{P_j^m})^{a_i}$.

Where,

P_j^m = mean partial pressure of the component j, atm

This centering procedure eases the parameter search by minimizing the statistical correlation between activation energy and pre-exponential factor [64, 65]. Thus, the reparameterized rate equation is given by

$$r_i = k_{io} \exp[\frac{-E_i}{R}(\frac{1}{T} - \frac{1}{T_m})]\left(\frac{P_j}{P_j^m}\right)^{a_i}\left(\frac{P_k}{P_k^m}\right)^{b_i} \qquad (3.22)$$

Table 3.1 Composition and Nomenclature of TiO_2 supported Cr-P-O catalysts

Nomenclature	Cr : P molar ratio	% Cr_2O_3 loading	%P_2O_5 loading
TiO_2	-	-	0
3CrTi	-	3	0
2Cr1PTi	2:1	2.96	1.38
1.5Cr1PTi	1.5:1	2.95	1.83
1Cr1PTi	1:1	2.92	2.72
1.4PTi	-	-	1.4

Table 3.2 Different Power Law models and corresponding number of kinetic parameters

Kinetic Model	Contributing reactions (Fig. 3.2)	Number of Parameters				
		k_{io}	E_i	a_i	b_i	Total
PL-1	$r_1, r_2, r_3.$	3	3	3	3	12
PL-2	r_1, r_4, r_5	3	3	3	3	12

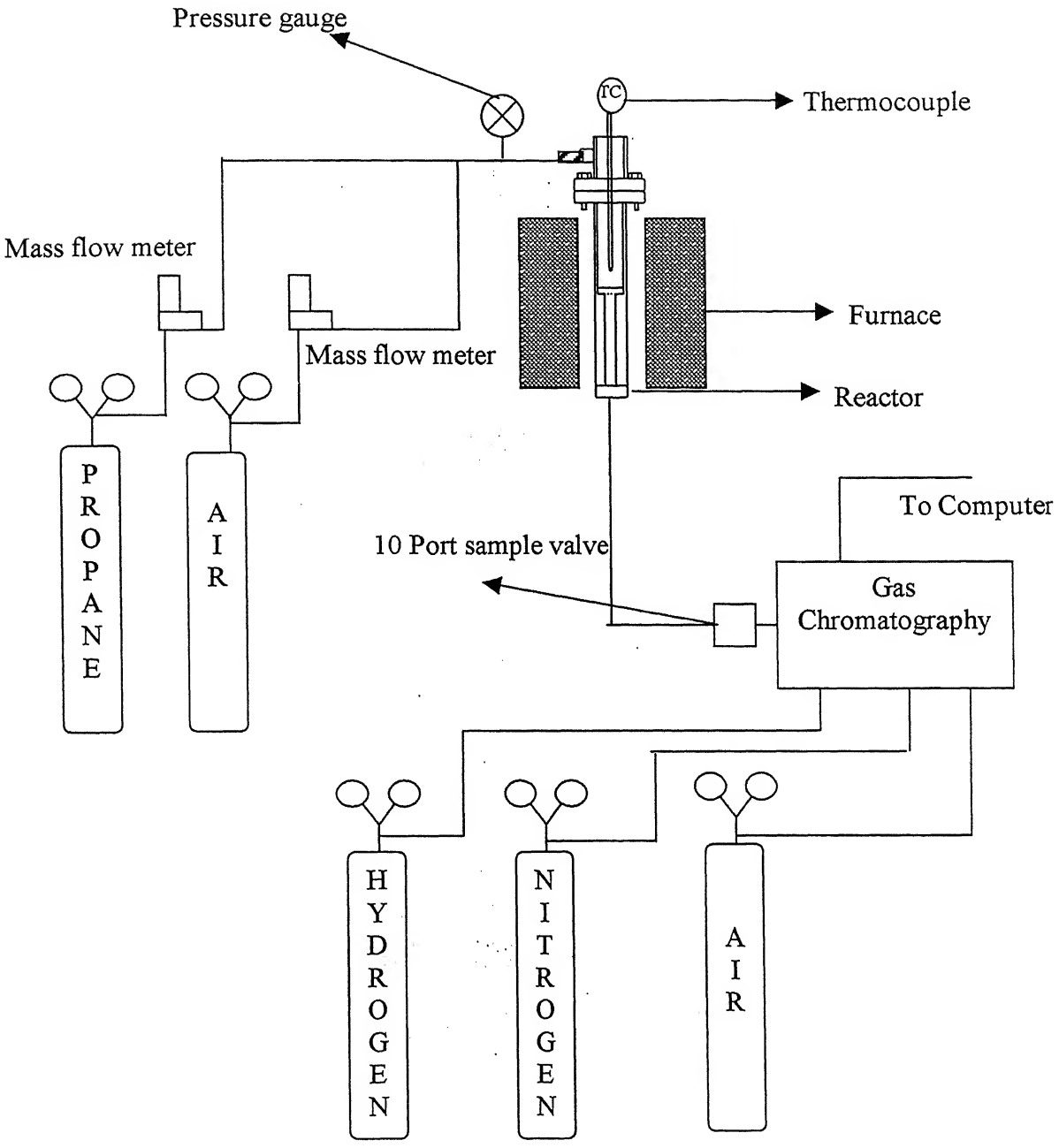

Figure 3.1 Reactor Setup

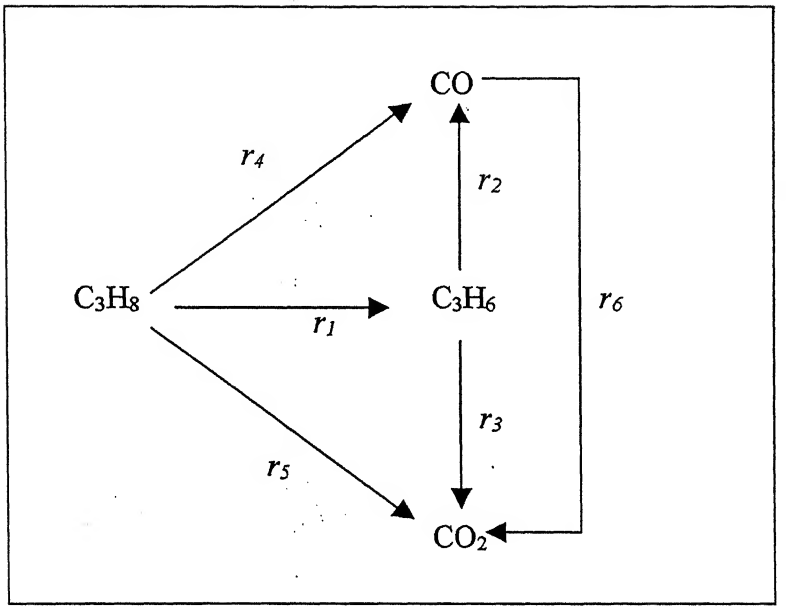

Figure 3.2 Generalized reaction network: Carbon containing molecules only shown

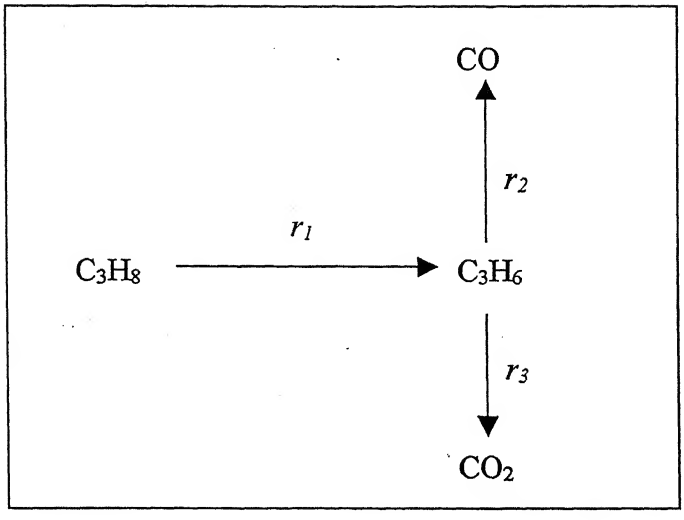

Fig 3.3 PL-1 reaction model

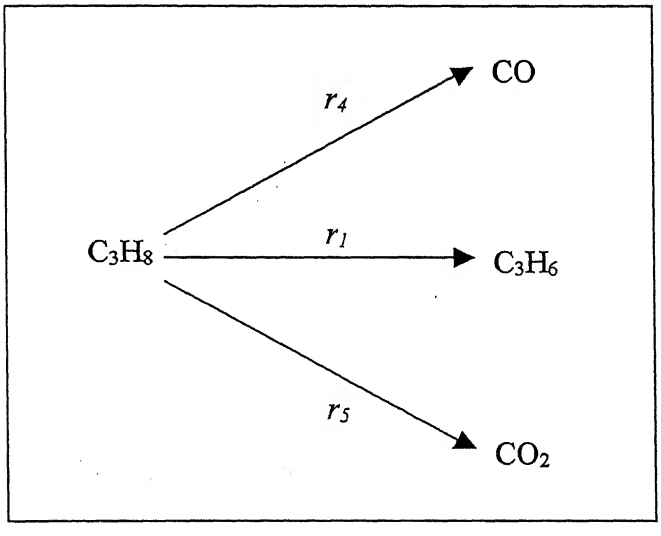

Fig 3.4 PL-2 reaction model

Chapter-4

Results and Discussion

Several unmodified and modified Cr_2O_3/TiO_2 catalysts were prepared. The unmodified catalysts contained 3 wt % of Cr_2O_3 on titania. The modified catalysts possessed ~ 3 wt % Cr_2O_3 and three different chromium to phosphorus molar ratios: 2:1, 1:5:1 and 1:1. In addition to these four samples, 3CrTi, 2Cr1PTi, 1.5Cr1PTi and 1Cr1PTi, another sample containing 1.4 wt% of P_2O_5 was also prepared. The BET surface areas of the prepared samples were initially obtained. The samples were further studied by XRD, EPR and TPR characterization techniques. The samples were then studied for the ODH of propane with the primary objective to understand the effect of phosphorus on the kinetic parameters. The results of these studies are summarized below.

4.1 Characterization Studies

4.1.1 Surface Area

The surface areas of the TiO_2 support, modified and unmodified chromia over titania samples were obtained and are tabulated in the second column of Table-4.1. Also included in Table 4.1 are results from TPR studies that are discussed later. It is observed that the surface areas were relatively constant (41 to 44 m^2/g) for modified and unmodified Cr_2O_3/TiO_2 samples and are slightly lower than the pre-treated pure support, 46 m^2/g. The decrease in surface area of samples may be due to the initial plugging of pores as suggested previously [66, 67]. Interestingly, when chromium oxide is deposited

on titania it gains stability against further decrease in surface area when the Cr_2O_3/TiO_2 sample is modified with phosphorus. Similar results were reported for vanadium oxide modified Cr_2O_3/ZrO_2 catalysts [68].

4.1.2 X-Ray Diffraction (XRD)

The XRD patterns of the titania support and supported samples are shown in Fig.1. For all the samples peaks are observed at 2θ values of 25.51, 27.61, 36.31, 38.16, 41.71, 48.26, 54.46, 55.26, 63.16, 69.36, 70.76, 75.71 and 76.31°. These peaks are due to the TiO_2 support. Consequently, other phases of chromium, phosphorus and/or titania are not detected by XRD. Small crystals of less than 40 nm size may still be present since they can not be detected by XRD. Similar conclusions are reported in the literature [69, 70].

4.1.3 Temperature Programmed Reduction (TPR)

The TPR profiles for unmodified and phosphorus modified chromia/titania (CrTi) along with phosphorus/titania (PTi) samples are shown in Fig. 4.2 where the TCD signal is plotted versus the temperature. It is observed from Fig. 4.2 that for all the phosphorus modified and unmodified CrTi samples two T_{max} temperatures were observed. The first reduction peak is observed at ~615 K and the second peak is observed to shift as the phosphorus content is increased. For 3CrTi the second reduction peak is at 736 K that shifts to 774 K for 2Cr1PTi, 809 K for 1.5Cr1PTi and 860 K for 1Cr1PTi. A high temperature reduction peak at 890 K is detected for 1.4PTi. The reduction peak at ~615 K, present in all chromia containing samples, corresponds to the reduction of the surface chromium oxide species [22]. Two reduction peaks were observed for Cr_2O_3/Al_2O_3 and

Cr_2O_3/SiO_2 samples also [71]. The T_{max} values for the samples are given in the third column of Table 4.1.

For quantitative analysis, the peak areas were integrated and the amount of hydrogen consumed was determined by injecting known amounts of hydrogen. From the calculated peak area of the first reduction peak and the calibration amounts of hydrogen, the hydrogen consumption is calculated. Based on the hydrogen consumed and the amount of chromia present the H/Cr molar ratio is calculated. The H/Cr ratios are tabulated in the fourth column of Table 4.1 for the unmodified and modified CrTi catalysts. From the data presented in Table 4.1, it appears that the first T_{max} temperature appears to be relatively constant. Furthermore, the H/Cr ratio appears to decrease with the addition of phosphorus to the CrTi catalyst suggesting that the amount of the surface chromium oxide species decreases.

4.1.4 Electron Paramagnetic Resonance (EPR)

The EPR spectra are obtained under ambient conditions for modified and unmodified chromia/titania samples and are shown in Figure 4.3. EPR spectroscopy is known to be sensitive to Cr^{5+} (d^1) and Cr^{3+} (d^3) cations and not to Cr^{6+} (d^0, diamagnetic) ions [72-75]. The catalyst free of phosphorus, i. e. the 3CrTi sample, exhibits typical strong axially symmetric peak with the parameters g=1.98 and ΔH= 50 G. This peak corresponds to the γ-signal of isolated axially symmetric Cr^{5+} species [76]. The Cr^{5+} species is also found in the EPR spectra of the phosphorus modified CrTi samples. On adding phosphorus to the CrTi sample, the γ-signal intensity decreases and a broad β-signal with g = 1.98 and Δ H = 820 G appears. This broad signal was also observed by Loukah et al. in characterizing

the $CrPO_4$ phase and was attributed to the presence of clustered Cr^{3+}-O-Cr^{3+} species in amorphous $CrPO_4$ [42]. The intensity of the β-signal increases with phosphorus addition. Consequently, with phosphorus addition the amount of Cr^{5+} species decreases and the amount of Cr^{3+}-O-Cr^{3+} species associated with amorphous $CrPO_4$ phase increases. No peak was found in the spectrum of 1.4PTi and is not shown.

Thus, characterization studies reveal that while preparing the catalyst the support is not significantly affected. Surface reducible chromia species are present in the modified and unmodified CrTi samples in addition to a Cr^{5+} and Cr^{3+} species associated with amorphous $CrPO_4$. The amount of surface reducible chromia species decreases and the Cr^{3+} species increases with an increase in phosphorus content.

4.2 ODH Reaction Studies

The propane ODH reaction with the unmodified and modified CrTi catalysts was performed. The unmodified and phosphorous-modified CrTi samples were observed to be active for the propane ODH reaction. Propene and carbon oxides (CO and CO_2) were the only reaction products detected. Titania and titania supported phosphorous were, however, inactive under the experimental conditions considered in the present study.

4.2.1. Contact Time Study

Initially, the propane ODH reaction was performed at a constant temperature of 653 K and a C_3H_8:O_2 molar flow ratio of 2:1. The flow rate was varied from 20 to 120 cc/min. The peak areas of C_3H_8, C_3H_6, CO_2 and CO obtained from the chromatographs are tabulated in Appendix-1. In each table there are six columns: the first column corresponds to the total flow rate in cc/min, the second column represents the contact

time (W/F_{Ao}) in Kg-m^{-3}s and the next four columns correspond to the peak area corresponding of C_3H_8, C_3H_6, CO_2 and CO, respectively.

Based on the areas the mole fractions of the components were determined from which the conversion and selectivity were calculated based on Eq. (3.1) and (3.2). The conversion and selectivity are used to generate Figs. 4.4. and 4.5. The propane conversion is plotted versus the contact time in Fig. 4.4. It is observed that for all of the catalysts the propane conversion increases with an increase in contact time. Furthermore, at a constant contact time the conversion decreases as the phosphorus amount in the catalyst increases. Thus, the activity follows the order 3CrTi>2Cr1PTi>1.5Cr1PTi>1Cr1PTi.

In Fig. 4.5 the propene selectivity is plotted against propane conversion. From Fig. 4.5 it is evident that the propane conversion and propene selectivity are inversely related. Furthermore, at iso-conversions the C_3H_6 selectivity increases with the amount of phosphorus in the catalyst except for the 1Cr1PTi sample where the selectivity decreases. Consequently, at iso-conversion the propene selectivity follows the order 1.5Cr1PTi>1Cr1PTi >2Cr1PTi>3CrTi. Thus, it appears that there exists an optimum Cr:P ratio where the selectivity, and, therefore the yield is maximum.

4.2.2. Reaction Data for Kinetic Investigation

The propane ODH was carried out over the active catalysts by varying the C_3H_8:O_2 molar ratio and temperature. The C_3H_8:O_2 ratio was varied as 3:1, 2:1 and 1:1 and the temperature was varied as 633, 653 and 673 K. During these reaction studies the total feed flow rate was maintained at 75 cc/min. All the runs were carried out in the

temperature range of 633 to 673 K. Each run was repeated twice to check the consistency of the result.

The raw peak areas of all the four analyzed components (CO, CO_2, C_3H_6 and unreacted C_3H_8) obtained during reaction over 3CrTi, 2Cr1PTi, 1.5Cr1PTi and 1Cr1PTi catalysts are presented in Appendix-2 as Tables A-2.1 to A-2.4, a separate table for each catalyst. In each table the first column corresponds to the C_3H_8:O_2 molar ratio. The second column of table provides the inlet area of propane, whereas the third column provides the temperature. The forth column of table represents the peak areas of the four analyzed components as obtained from the GC. The last column contains the carbon balance.

The peak areas shown in Appendix-2 are used to calculate the product (CO, CO_2 and C_3H_6) yields based on Eq. 3.3. The calculated yield values at all reaction conditions are presented in Table 4.2 to 4.5 for the four catalysts. The first column of the tables corresponds to the reaction temperature and the second column corresponds to the C_3H_8:O_2 molar ratio. The product yields obtained are given in the third column of the table and the last column gives the carbon balance (C-balance) in terms of the ratio of carbon atoms out to carbon atoms in, C_{out}/C_{in}. As mentioned previously the C-balance provides a measure of the accuracy of GC analysis. Examination of the C-balance values reveals that the GC- analysis is reliable. Analysis of the yield values of Table 4.2 to 4.5 reveals that for all the catalysts the C_3H_6, CO_2 and CO yields increase with an increase in temperature. However, at a particular temperature the yields are decreasing with an increase in C_3H_8:O_2 molar ratio. Comparison of the yield values of one catalyst with another is not possible since the weight of the catalysts, and, consequently, the contact

times and conversions are different. Comparison of the yields at iso-conversion or the same contact time is more appropriate and is done based on the kinetic parameters estimated.

4.3. Kinetic Parameter Estimation

Based on the inlet C_3H_8 and O_2 concentrations and outlet areas detected by GC (Appendix-2), the input and output mole percents of different components are calculated and shown in a tabular form in Appendix-3. There are four tables in Appendix-3 from A-3.1 to A-3.4 corresponding to the four catalysts. The first column in the tables corresponds to the reaction temperature, while the second and third columns give the input (C_3H_8 and O_2) and output (C_3H_8, C_3H_6, CO_2 and CO) mole percents. The data in each table is organized such that the C_3H_8:O_2 molar ratio of 1:1 is the top set of the data, and is separated by a bold line from the following C_3H_8:O_2 ratio of 2:1 data, which is followed by the C_3H_8:O_2 ratio of 3:1 data. In each data set, corresponding to particular C_3H_8:O_2 molar ratio, the data is presented with increasing reaction temperature from 633 to 673 K.

Based on the input and output mole percents of C_3H_8, C_3H_6, CO_2 and CO, the kinetic parameters for the four catalysts based on PL-1 and PL-2 models, discussed in section 3.6, are determined by minimizing the objective function. As mentioned before in the section 3.3.2 a determinant was used as the objective function.

4.3.1. Model Selection

After estimating the parameters comparison of the PL-1 and PL-2 is done. Since the number of parameters used in the PL-1 and PL-2 models are the same comparison of

the determinant values used as the optimization criteria would provide the better suitability of the model to explain the reaction data. The determinant value (D. V.) for all the four catalysts obtained from PL-1 and PL-2 is presented in Table 4.6. Invariably the D. V. is smaller for the PL-1 than the PL-2 model for all the catalysts. Consequently, it appears that the PL-1 model explains the experimental data better than the PL-2 model. The PL-1 model suggests that a consecutive reaction takes place where carbon oxides are secondary products and propene is the only primary product. Similar conclusions have been previously proposed [49].

4.3.2. Kinetic parameters for the PL-1 model

The kinetic-parameters of the PL-1 model, consisiting of pre-exponential factors, k_{i0}, activation energy, E_i, and partial pressure exponents, a_i & b_i, are determined for the 3CrTi, 2Cr1PTi, 1.5Cr1PTi and 1Cr1PTi catalysts and are presented in Table 4.7. For determining the kinetic parameters the values of $P_{m(C_3H_8)}$ = 0.2958 atm, $P_{m(O_2)}$ = 0.148 atm and T_m = 653.16 K are considered. The units of the parameters are also presented in the tables. The last row of Table 4.7 corresponds to the $P_{m(C_3H_6)}$, which is different for each catalyst. Despite PL-2 being less suitable for the present study, kinetic parameters are presented in Appendix-4.

Using the kinetic parameters of PL-1 model and the experimental conditions used, the outlet concentration of C_3H_8, C_3H_6, CO_2 and CO can be predicted. To show the proper estimation of kinetic-parameters, the predicted outlet concentrations of C_3H_6, CO_2 and CO are compared with the actual outlet concentrations in Fig. 4.6. From the figure it is clear that the kinetic parameters estimated for the PL-1 model is effective in

representing the propane ODH reaction under the experimental conditions used in the present study.

The effect of phosphorus addition on Cr_2O_3/TiO_2 is analyzed by comparing the kinetic-parameters of the four catalysts. By examining the k_{10} values for the unmodified and modified catalysts in Table 4.7 reveals that the magnitude of the k_{10} values decreases from 3.74 for 3CrTi to 1.68 for 1Cr1PTI as phosphorus is added. The k_{20} also decreases monotonically with phosphorus addition. The k_{30} value decreases for the 3CrTi, 2Cr1PTi and 1.5Cr1PTi catalysts as phosphorus is added and increases for the 1Cr1PTi catalyst. For each of the catalysts $k_{10} > k_{30} > k_{20}$ except for 3CrTi where $k_{10} < k_{30} > k_{20}$. Creaser and Anderson have also observed similar trend in k_{10}, k_{20} and k_{30} for the propane ODH reaction over a VMgO catalyst [49].

To understand the variation of k_{i0} values with phosphorus addition, the k_{i0} values are normalized with the k_{i0} values of the 3CrTi catalyst and are plotted in Fig. 4.7 for the four catalysts. The normalized k_{io} decreases with the addition of phosphorus except for the normalized k_{30} value, which initially decreases and then increases for the 1Cr1PTi catalyst. However, the relative decrease of the k_{i0} values is not the same for all the catalysts. The normalized k_{10} value decreases and appears to approach a relatively constant value. The normalized k_{20} value decreases more rapidly and almost linearly with phosphorus addition. The normalized k_{30} value decreases the most rapidly and finally increases for the 1Cr1PTi sample. Thus, the pre-exponential factors do not decrease at the same rate with phosphorus addition. Consequently, the pre-exponential

factors for the propane dehydrogenation reaction and propane combustion reaction are affected differently with phosphorus addition.

The pre-exponential factors are specific to the catalytic active site and depend on the activity per site or the number of active sites. Relating this information with characterization studies suggest that the number of active sites is affected since the H/Cr ratio associated with the surface chromium oxide species and the EPR spectra also changes. The characterization studies suggest that the surface chromia species are less and a new Cr^{3+} species associated with the $CrPO_4$ related phase is present. The decrease in the k_{io} values with phosphorus addition appears to be related to the decrease in the surface chromium oxide species. The increase in the k_{30} value for the 1Cr1PTi catalyst appears to be related to the formation of a new chromium oxide phase.

The ranges of activation energy given in Table-4.7 for propane ODH, E_1, are from 123 to 165 kJ/mol; for propene combustion to CO, E_2, are from 24 to 55 kJ/mol; for propene combustion to CO_2, E_3, are from 22 to 61 kJ/mol. The relative trends of the activation energies values are consistent with previous studies that suggested E_2 and E_3 should be less than E_1 [47, 49, 51]. The difference in activation energies for ODH and combustion are important for obtaining high propene yields. A plot of E_1-(E_2+E_3) for the four catalysts is shown in Fig. 4.8. It is observed from the figure that the difference in activation energy for propane ODH and propene degradation is relatively constant for 3CrTi, 2Cr1PTi and 1.5Cr1PTi, but significantly different for the 1Cr1PTi sample, consistent with the formation of new phase.

The partial pressure exponents, a_i and b_i, for all the catalysts are also given in the Table 4.7. A pseudo-first order dependency of propane for r_1 is observed for 2Cr1PTi and

1.5Cr1PTi, whereas r_1 appears to be independent of propane partial pressures for 3CrTi and 1Cr1PTi samples. The oxygen dependency for the primary reaction r_1 is first order for most catalyst. The rate of CO formation is independent of oxygen partial pressure except for the case of 2Cr1PTi where it follows a first order dependency. No specific trend is observed for the other exponent values. In general, it appears that there is no common reactant partial-pressure dependency for all the catalysts. Each catalyst has its specific partial pressure dependency.

Thus, the kinetic parameters of the reactions involved in both PL-1 and PL-2 models were successfully determined using GA for the unmodified and phosphorus-modified chromia over titania catalysts. The most suited model suggests that propene is a primary product, which then degrades to carbon oxides. Phosphorus addition primarily affects the pre-exponential factors, whereas the activation energies and partial pressure exponents are not affected or affected randomly.

4.4. Predicted Yield

Based on the estimated kinetic-parameters the effect of conversion on propene yield and selectivity can be determined. Using the kinetic parameters and for reaction conditions of C_3H_8:O_2 molar ratio of 2:1 the calculated propene yield versus contact time at reaction temperatures of 633, 653, 663 and 673 K are plotted in Fig. 4.9 for the 3CrTi catalyst. From Fig. 4.9 it is observed that a specific contact time exists for maximum propene yield. Furthermore, as the temperature increases the propene yield also increases. With an increase in temperature, the ratio of the rate constants for propene degradation to propane ODH, $(k_2+ k_3)/k_1$, also decreases. Similar behavior is also observed for first order consecutive reactions where the optimum yield of the intermediate product increases as

the ratio of the rate constants of the first and second reaction decreases [77]. In the present study the change of the ratio between the rate constants can be brought about a change in temperature and change in catalyst composition.

In Fig. 4.10 the calculated propene yield is plotted versus conversion at 653K and again an optimum is observed except for the 2Cr1PTi catalyst. For the 2Cr1PTi catalyst the propene yield monotonically increases with conversion. Furthermore, from Fig. 4.10 the optimum propene yield increases as the $(k_2+k_3)/k_1$ ratio decreases except for the 2Cr1PTi where an optimum propene yield is not observed. In comparison to Fig. 4.9, in Fig. 4.10 the decrease in $(k_2+k_3)/k_1$ ratio is achieved by changing the catalyst composition. Addition of phosphorus to the CrTi catalyst decreases the $(k_2+k_3)/k_1$ ratio to a minimum value for 1.5Cr1PTi. The $(k_2+k_3)/k_1$ increases again for the 1Cr1PTi catalyst.

The selectivity is plotted versus conversion in Fig. 4.11 for all the four catalysts. The predicted selectivity versus conversion curves reveals that an inverse relationship exists between the conversion and selectivity. Furthermore, at iso-conversion the propene selectivity increases with phosphorus addition except for 1Cr1PTi sample where the selectivity decreases. Similar trends are observed in contact time studies in Fig. 4.5 also where the propene selectivity was maximum for 1.5Cr1PTi catalyst.

Thus, the propene yield can be controlled to some extent by the reaction temperature and catalyst composition. With an increase in temperature the ratio of the rate constant associated with degradation to the rate constant associated with ODH decreases. The decrease in rate constant ratios results in a higher propene yield. An increase in propene yield can also be achieved by phosphorus addition since the rate constants ratio of degradation to ODH also decreases till an optimum Cr:P ratio of 1.5:1.

The decrease in propene yield for Cr:P ratio less than 1.5:1 appears to be related to the increase in the pre-exponential value associated with propene degradation to CO_2. Interestingly, for C_2H_6 ODH an optimum ratio of P:Cr of 1.6 was found by Ziyad et al. [38]. Thus, the optimum Cr:P ratio appears to depend on the ODH of the specific alkane.

Table-4.1: Surface area (S. A.), T_{max} and H/Cr ratio of the catalysts

Catalysts	S. A., (m^2/g)	T_{max} (K)	H/Cr (molar ratio)
TiO_2	46	-	-
3CrTi	42	612, 736	1.21
2Cr1PTi	44	613, 774	0.96
1.5Cr1PTi	44	613,809	0.81
1Cr1PTi	43	619, 860	0.44
1.4PTi	41	890	-

Table 4.2: Product yield obtained with 3CrTi catalyst for propane ODH

Weight of the catalyst = 0.20 g; Total flow rate =75cc/min.

Reaction Temperature (K)	C_3H_8/O_2 ratio	Yield (%)			C-balance (C_{out}/C_{in})
		C_3H_6	CO_2	CO	
633	1:1	0.49	0.46	0.15	0.990
	2:1	0.30	0.44	0.10	0.996
	3:1	0.22	0.30	0.08	0.996
653	1:1	1.40	1.11	039	0.956
	2:1	0.72	0.8	0.23	0.998
	3:1	0.48	0.42	0.13	0.993
673	1:1	3.97	2.31	1.29	0.917
	2:1	1.29	0.91	0.38	0.989
	3:1	1.21	0.71	0.37	0.974

Table 4.3: Product yield obtained with 2Cr1PTi catalyst for propane ODH

Weight of the catalyst = 0.20 g; Total flow rate = 75cc/min.

Reaction Temperature (K)	C_3H_8/O_2 ratio	Yield (%)			C-balance (C_{out}/C_{in})
		C_3H_6	CO_2	CO	
633	1:1	0.26	0.15	0.07	0.993
	2:1	0.23	0.10	0.06	1.002
	3:1	0.21	0.07	0.05	0.999
653	1:1	0.62	0.28	0.13	1.014
	2:1	0.45	0.27	0.15	0.999
	3:1	0.43	0.17	0.11	0.994
673	1:1	1.33	0.40	0.22	1.013
	2:1	1.09	0.49	0.31	0.989
	3:1	0.76	0.34	0.24	0.996

Table 4.4: Product yield obtained with 1.5Cr1PTi catalyst for propane ODH Weight of the catalyst = 0.20 g; Total flow rate =75cc/min.

Reaction Temperature (K)	C_3H_8/O_2 ratio	Yield (%)			C-balance (C_{out}/C_{in})
		C_3H_6	CO_2	CO	
633	1:1	0.26	0.10	0.05	0.998
	2:1	0.23	0.07	0.05	0.984
	3:1	0.19	0.07	0.05	0.998
653	1:1	0.34	0.22	0.10	0.987
	2:1	0.37	0.12	0.08	0.973
	3:1	0.36	0.14	0.09	0.979
673	1:1	0.92	0.35	0.19	0.828
	2:1	0.84	0.28	0.19	0.973
	3:1	0.60	0.25	0.18	0.982

Table 4.5: Product yield obtained with 1Cr1PTi catalyst for propane ODH Weight of the catalyst = 0.20 g; Total flow rate =75cc/min.

Reaction Temperature (K)	C_3H_8/O_2 ratio	Yield (%)			C-balance (C_{out}/C_{in})
		C_3H_6	CO_2	CO	
633	1:1	0.18	0.08	0.02	0.992
	2:1	0.12	0.02	0.02	0.953
	3:1	0.07	0.01	0.01	0.991
653	1:1	0.36	0.15	0.03	0.992
	2:1	0.24	0.03	0.03	0.944
	3:1	0.13	0.02	0.02	0.966
673	1:1	0.49	0.20	0.04	0.996
	2:1	0.41	0.07	0.06	0.922
	3:1	0.26	0.04	0.03	0.922

Table 4.6: Determinant values obtained during kinetic parameter estimation from PL-1 and PL-2 Model

Catalyst	Determinant Value	
	PL-1	PL-2
3CrTi	5.69e-27	3.3e-26
2Cr1PTi	3.05e-31	9.8e-29
1.5Cr1PTi	4.06e-29	6.6e-28
1Cr1PTi	5.92e-28	5.9e-27

Table 4.7: Kinetic parameters for PL-1 model

Calculated at $P_{m(C_3H_8)}$ = 0.2958 atm, $P_{m(O_2)}$ = 0.148 atm, T_m = 653.16 K

Parameter	Units	Catalyst			
		3CrTi	2Cr1PTi	1.5Cr1PTi	1Cr1PTi
k_{10}	$ml\ STP\ min^{-1}\ (g\ cat)^{-1}\ atm^{-(a1+b1)}$	3.74	2.75	1.78	1.64
k_{20}		0.77	0.51	0.30	0.10
k_{30}		4.12	1.35	0.70	1.37
E_1	$kJ\ mol^{-1}$	156	145	165	123
E_2		45	24	55	52
E_3		26	22	40	61
a_1	*Dimensionless*	0.18	1.0	1.0	0.01
b_1		1.0	0.83	1.0	1.0
a_2		1.0	0.01	0.58	0.35
b_2		0.01	1.0	0.01	0.01
a_3		0.39	0.79	0.09	0.58
b_3		0.57	1.0	0.01	0.55
$P_{m(C_3H_6)}$	*atm*	0.0015	9.9E-04	5.2E-04	2.6E-04

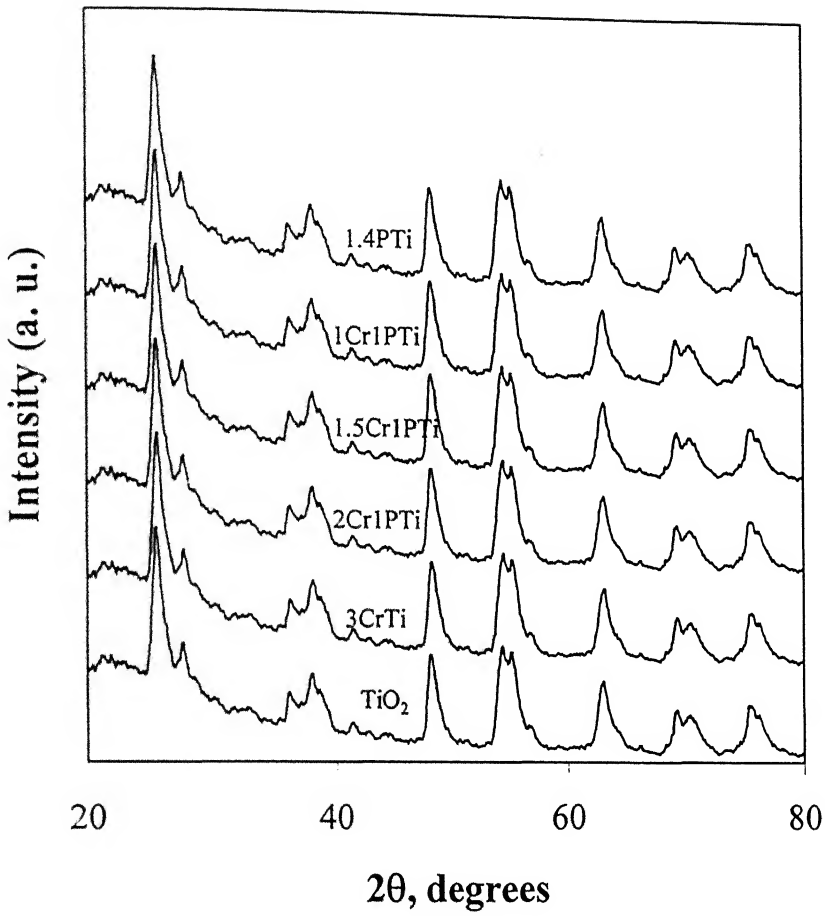

Figure 4.1: X-Ray diffractograms of TiO_2, 3CrTi, phosphorus modified CrTi and 1.4PTi samples

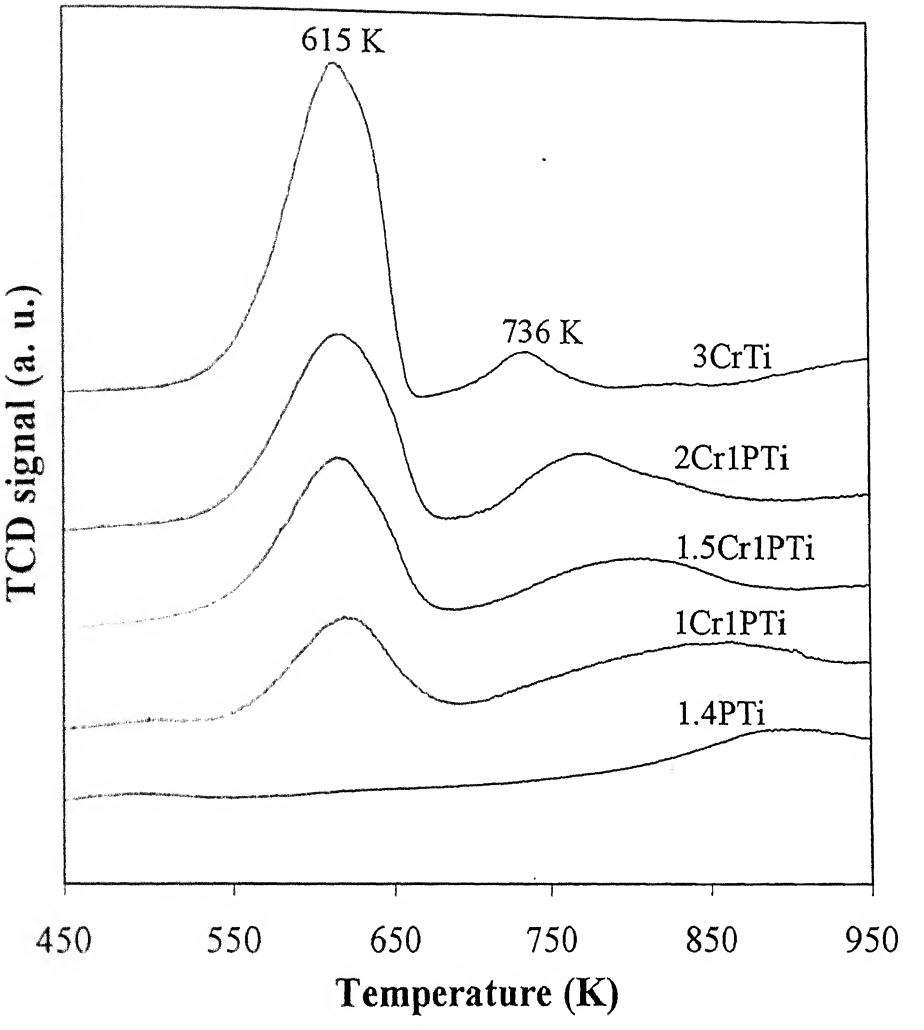

Figure 4.2: TPR profile for unmodified 3CrTi, phosphorus modified CrTi and 1.4PTi

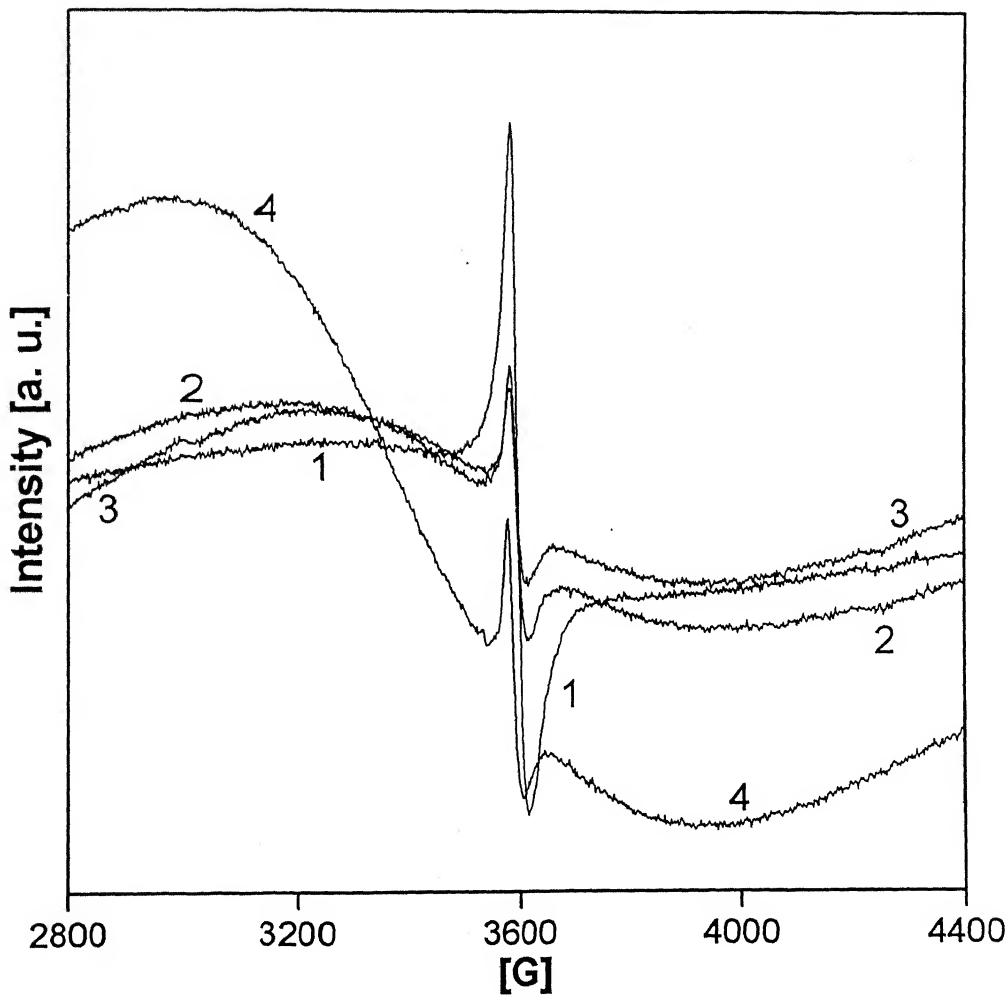

Figure 4.3: EPR spectra of catalyst samples under ambient conditions

Legends: 1- 3CrTi 2- 2Cr1PTi

3- 1.5Cr1PTi 4- 1Cr1PTi

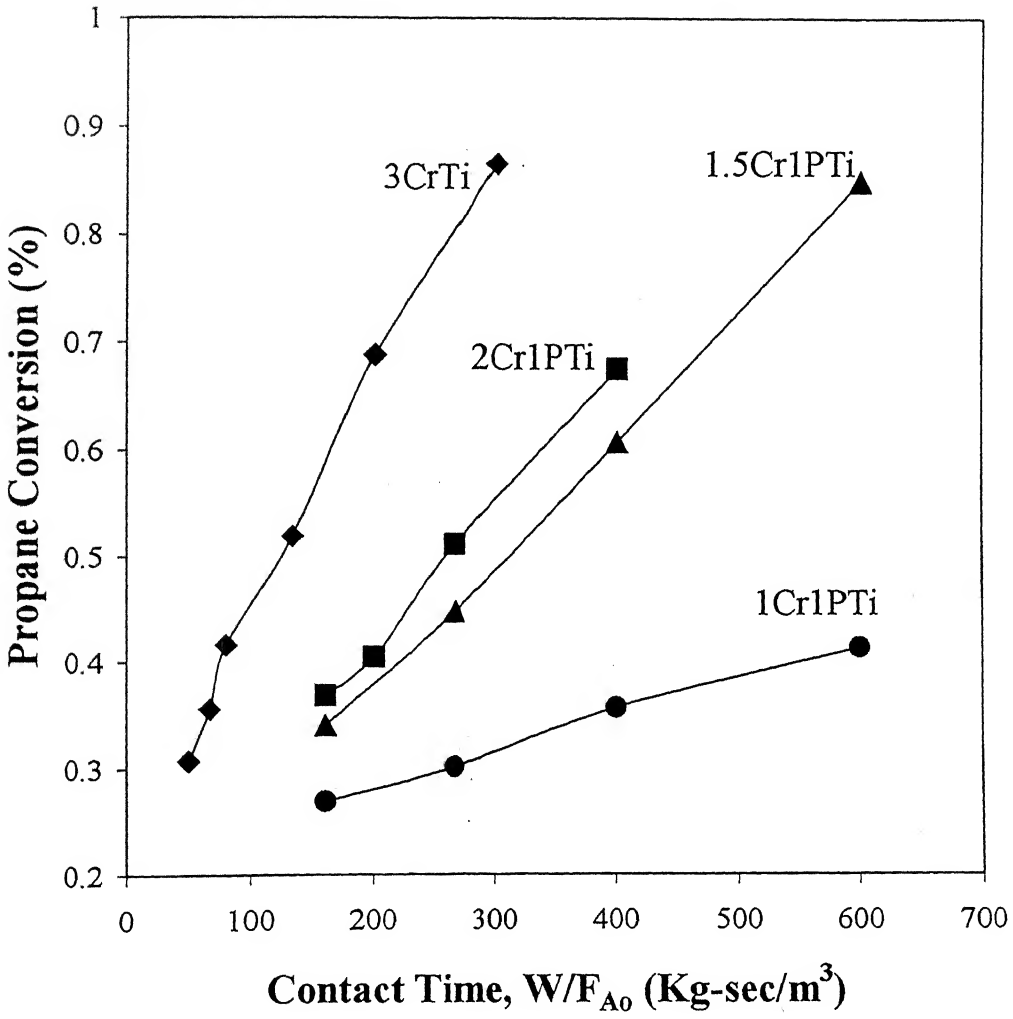

Figure 4.4: Propane conversion versus contact time for unmodified and phosphorus modified CrTi

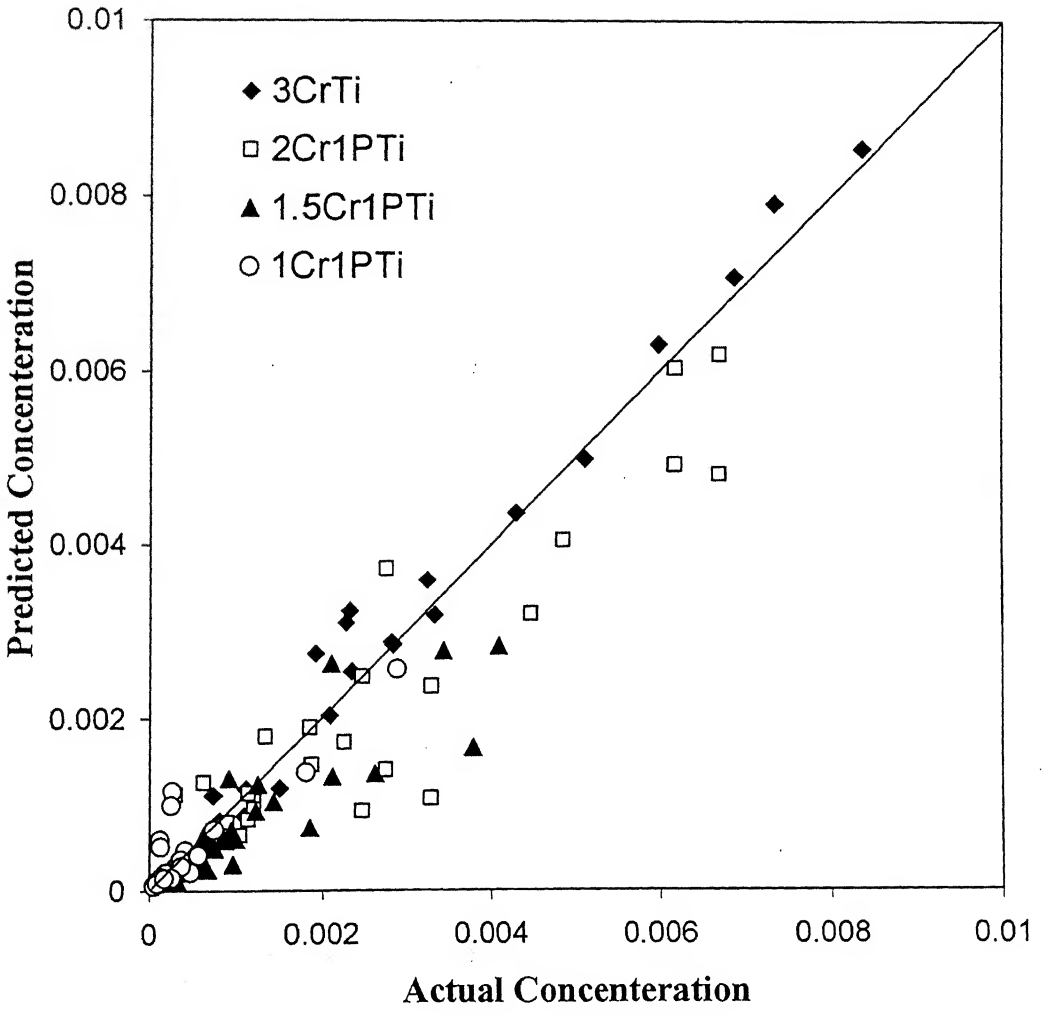

Figure 4.6: Actual concentration versus predicted concentration using PL-1 model for unmodified and phosphorus modified CrTi

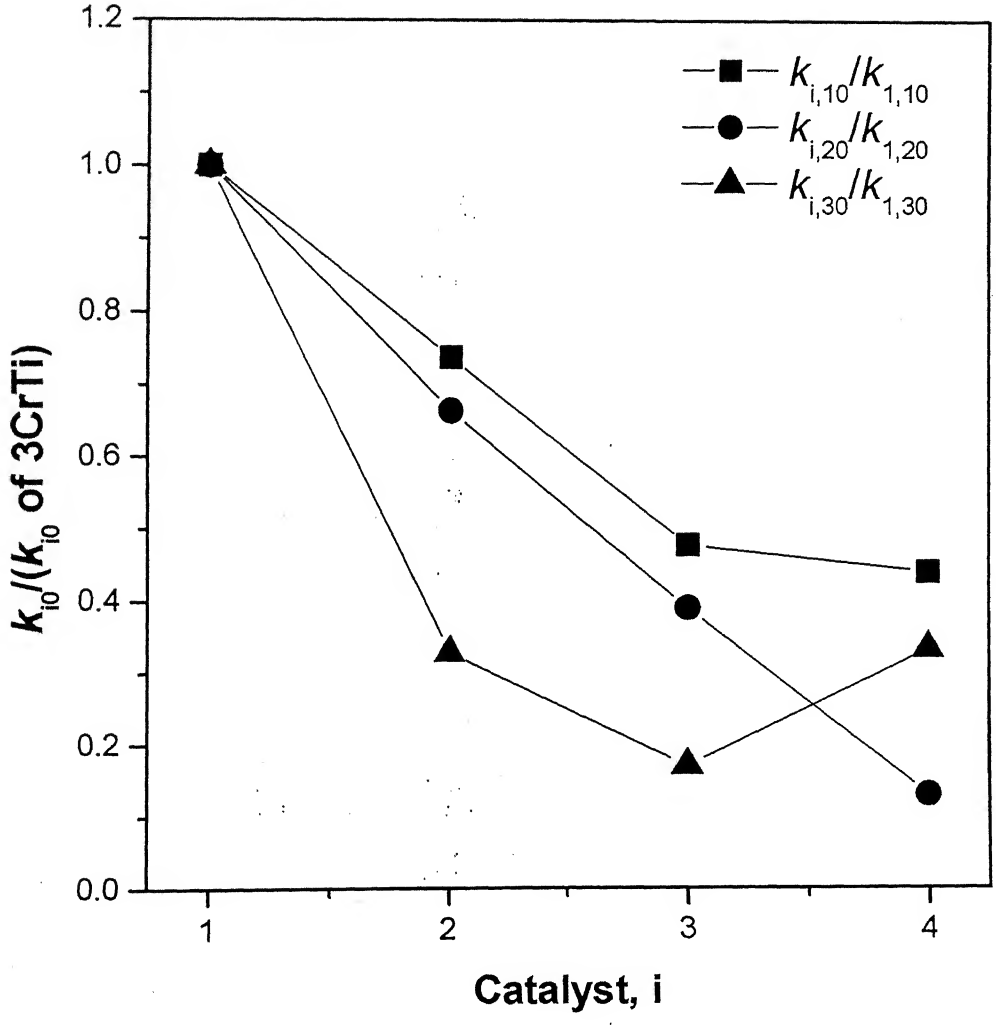

Figure 4.7: Normalized k'_{i0} for all the catalysts

Legends, i (on x-axis): 1-3CrTi 2-2Cr1PTi

3-1.5Cr1PTi 4-1Cr1PTi

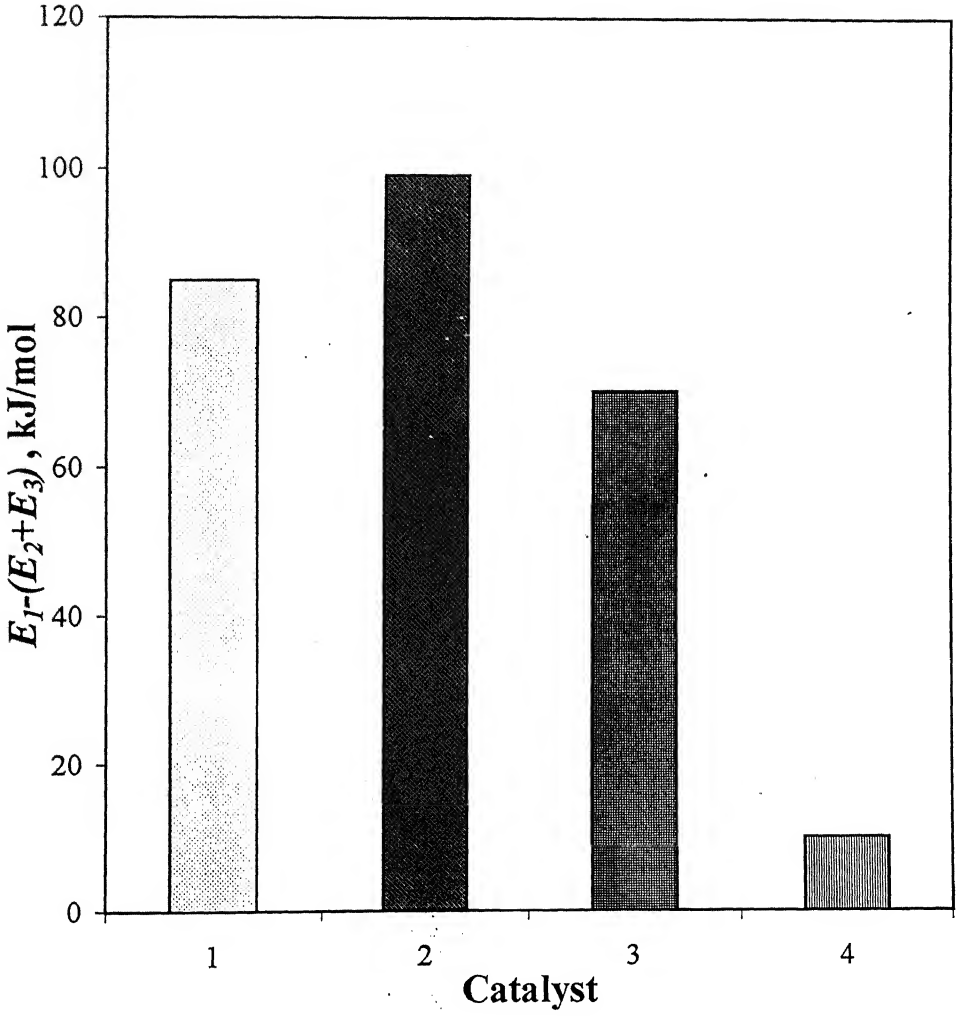

Fig. 4.8: Difference in activation energies of propane ODH and propene degradation

Legends, (on x-axis): 1-3CrTi 2-2Cr1PTi 3-1.5Cr1PTi 4-1Cr1PTi

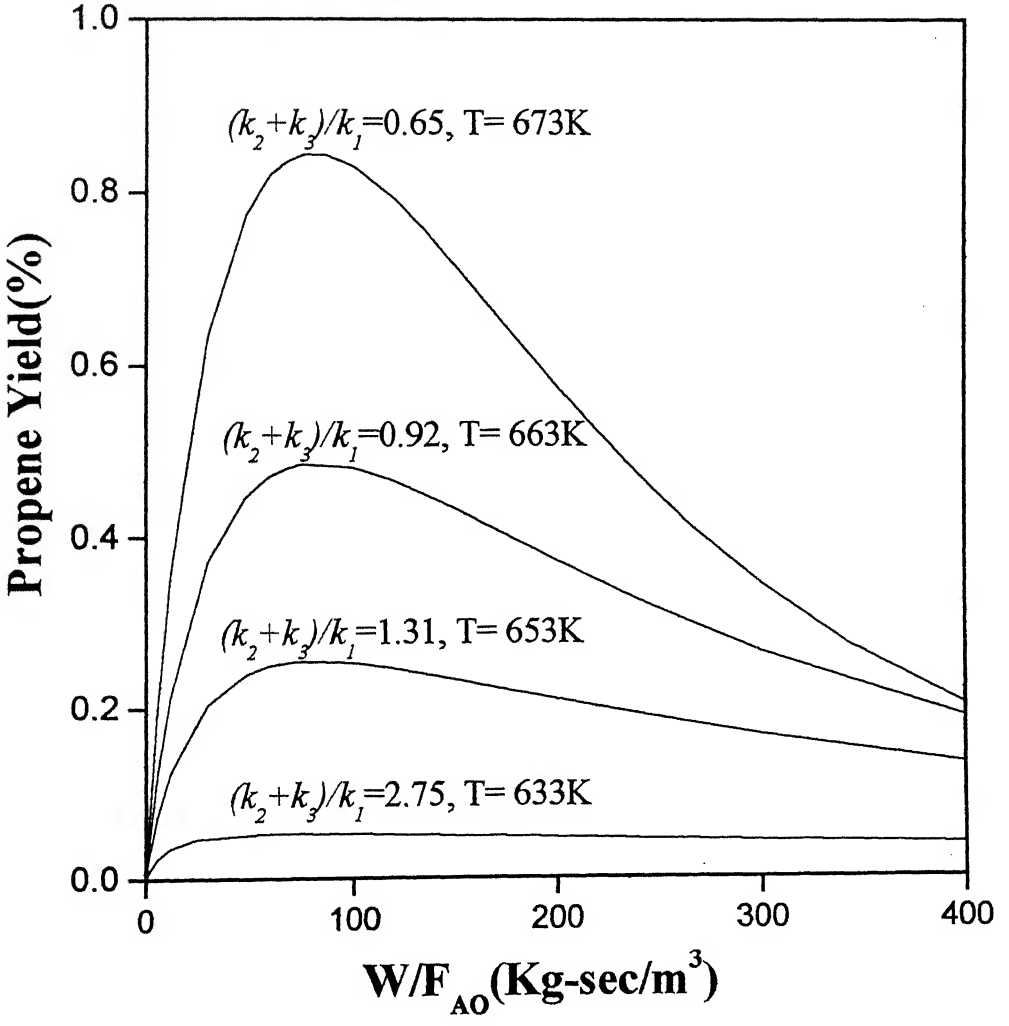

Figure 4.9: Predicted propene yield versus contact time for 3CrTi catalyst; wt. of catalyst=0.2g, C_3H_8 : O_2 = 2:1.

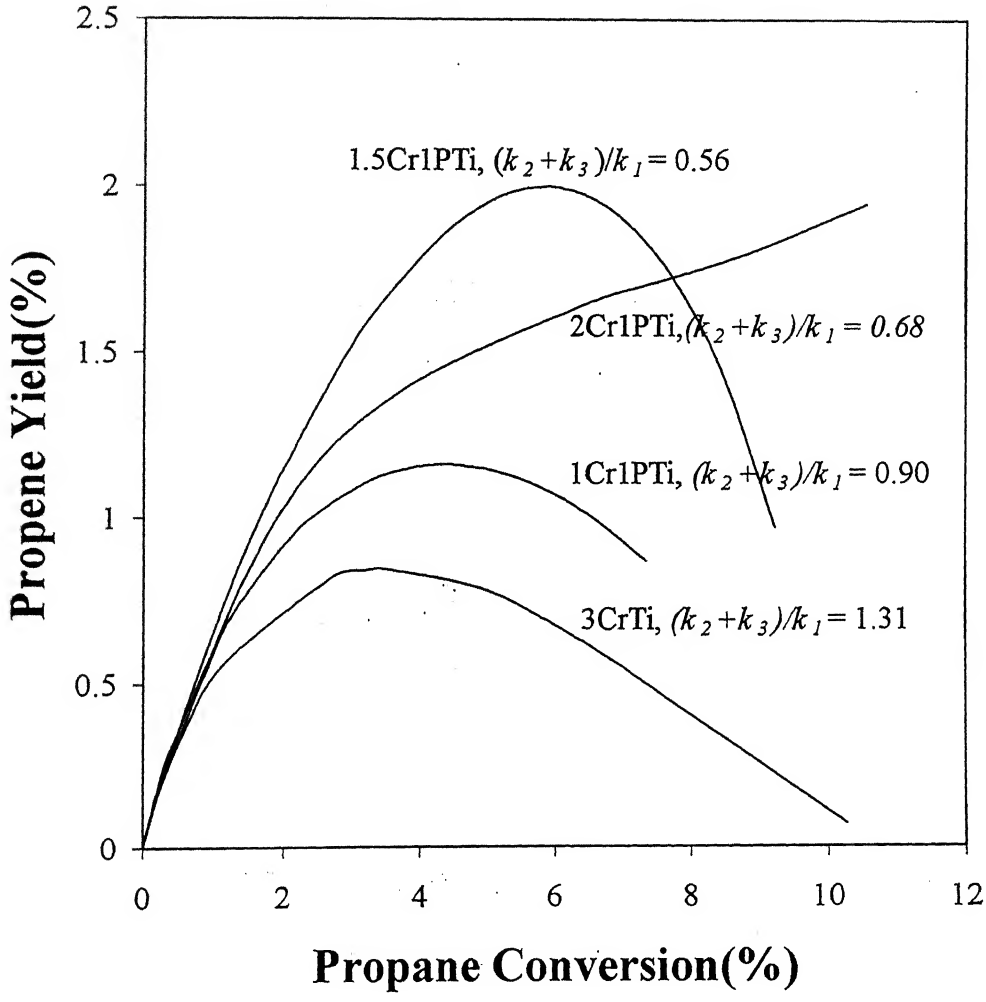

Figure-4.10: Predicted propene yield versus propane conversion for unmodified and phosphorous modified CrTi samples. Temperature = 653 K; C_3H_8 : O_2 = 2:1.

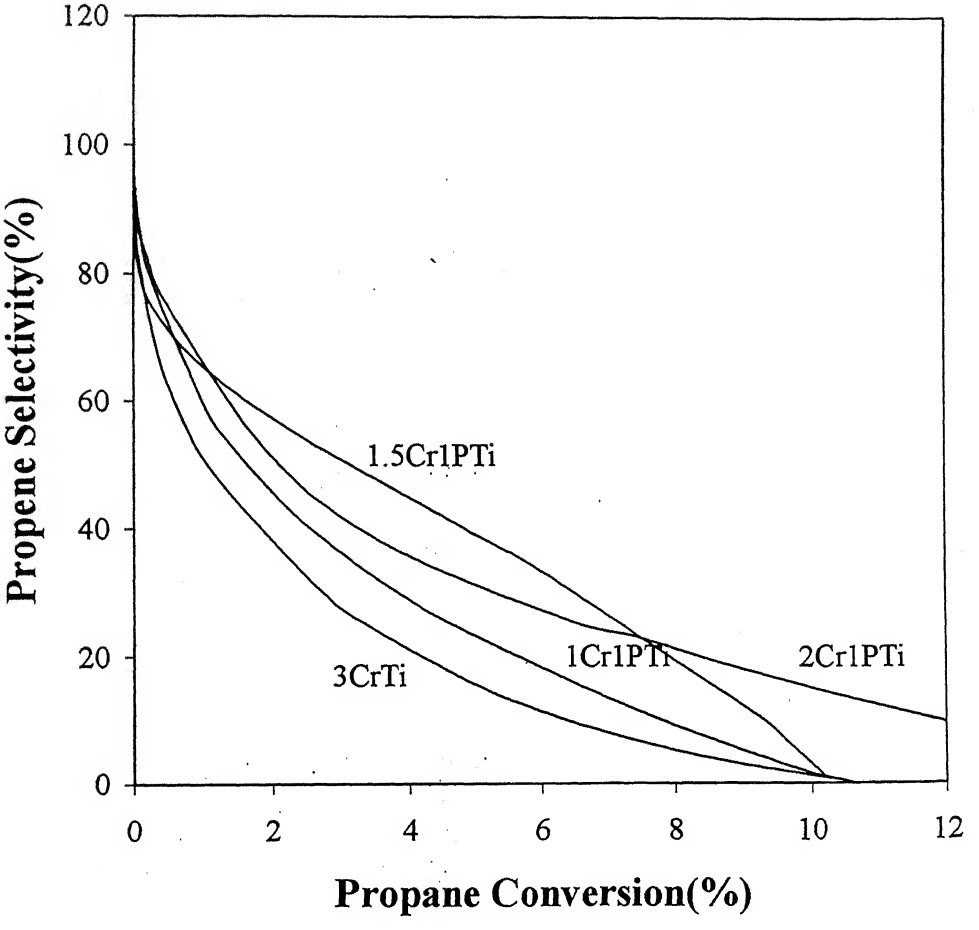

Figure-4.11: Predicted propene selectivity versus propane conversion for unmodified and phosphorous modified CrTi samples. Temperature = 653 K; C_3H_8 : O_2 = 2:1.

Chapter: 5

Conclusions and Recommendations

5.1. Conclusions

The effect of phosphorus modification on the structure and reactivity of the 3% Cr_2O_3/TiO_2 sample was studied by initially synthesizing four catalysts, by applying various characterization techniques (surface area, XRD, TPR and EPR) and finally carrying out the ODH of propane reaction.

The surface area and XRD results revealed that the TiO_2 support structure is not significantly affected with deposition of chromia and/or phosphorus. In the XRD analysis no new crystalline phase was detected suggesting that no new compounds were formed. The TPR studies gave two peaks due to the reduction of surface chromate group. The first reduction peak at ~615K corresponds to the reduction of the surface Cr^{6+} species. The peak area associated with the surface chromium oxide species decreased with the phosphorus addition suggesting that the surface Cr^{6+} species is progressively poisoned. Peaks due to γ-Cr^{5+} and clustered Cr^{3+}-O-Cr^{3+} in amorphous $CrPO_4$ were observed in the EPR spectra. The amount of Cr^{3+} due to the amorphous $CrPO_4$ increases with phosphorus addition.

The ODH of propane was performed with unmodified and phosphorus modified CrTi samples to examine its catalytic behavior. The propene selectivity was observed to increase and reach a maximum for a Cr:P ratio of 1.5 and then decrease with phosphorus modification. The conversion, however, decreased monotonically with phosphorus modification.

Two power law models were considered to explain the experimental data. The best suited power law model suggested propene as a primary product and carbon oxides as secondary product formed by propene degradation. The pre-exponential factors obtained for this model decreased with phosphorus addition (except for k'_{30} for 1Cr1PTi) at different rates, which was due to the decrease in number of active sites. The activation energies for the propene degradation to CO and CO_2 were found to be less than that of propane ODH. No specific trend in partial pressure exponents is observed as an effect of phosphorus addition to Cr_2O_3/TiO_2 catalyst. Based on the kinetic-parameters the propene yield was predicted and observed to be highest for 1.5Cr1PTi catalyst, which possessed the lowest $(k_2+k_3)/k_1$ value. Thus, controlling the $(k_2+k_3)/k_1$ by changing the catalyst composition will give rise to increased propene yields.

5.2. Recommendations

Based on the observations and conclusions of the present study, the following recommendations can be made:

1. More detailed characterization of the modified catalysts using other techniques, such as XPS, DRS, dehydrated Raman spectroscopy and electron microscopy should be performed to obtain better insight into the nature of the catalysts.
2. Preparation of the modified catalysts should be in various sequences, i. e., deposition of the active species to the modified-support or deposition of the modifier (phosphorus) to the supported catalysts, in order to understand the effect of preparation sequence on the structure-reactivity of the modified catalysts.

3. Mechanistic models, such as Langmuir-Hinselwood and Eley-Rideal and Redox models should also be carried out for predicting the reaction pathways of propane to propene and for the better understanding of the reaction mechanism.
4. Use of other modifiers to observe if the propene yield can be increased further.

References

1. H.H. Kung, *Advances in Catalysis*, 40 (1995) 1.
2. J. Gascon, C.Tellez and J. Herguido and M. Menendez, *Applied Catalysis, A: General* (2003), 248(1-2), 105-116.
3. S. M. K Airaksinen, J. M Kanervo and A. O. I Krause, *Studies in Surface Science and Catalysis* (2001), 136(Natural Gas Conversion VI), 153-158.
4. F. Cavani and F. Trifiro, *Catalysis Today*, 24 (1995) 307-313.
5. M. Che, O. Clause and Ch. Marcelly, *Hand Book of Heterogeneous Catalysis*, Vol. 2 (1997) 191.
6. F. D. Hardcastle and I.E. Wachs, *J. Mol. Catal.*, 46 (1988) 173.
7. A. J. van Hongstum, J. Pranger, J. G. van Ommen and P. J. Gellings, *Applied Catalysis A: Gen.*, 11 (1984) 317.
8. I. E. Wachs, R. Y. Saleh, S. S. Chan and C. Chersich, *CHEMTECH*, Dec. (1985) 758.
9. I. E. Wachs, *Catalysis Today*, 27 (1996) 437.
10. I.E. Wachs, G.Deo, D. S. Kim, M.A. Vuurman, and H. Hu, "*Molecular design of supported metal oxide catalysts*", Preprint of the 10th international conference in catalysis, Budapest (Hungry), 1992, p 72.
11. R. Grabowski, B. Grzybowska, J. Stoczynki and K. Wcislo, *Applied Catalysis A: Gen:* 144 (1996) 335.
12. M. Hoang, J.F. Mathew and K.C. Pratl. *React. Kinet.Catal. Lett.*, 61 (1997) 21.

13. S. De Rossi, G. Ferraris, S. Fremiotti, A. Cimino and V. Indovina, *Applied Catalysis A: Gen,* 81 (1992) 113.

14. D. W. Flick and M.C. Huff, *Applied Catalysis A: Gen.*, 187 (1999) 13.

15. S. Wang, K. Murata, T. Hayakawa, S. Hamakawa and K. Suzuki, *Applied Catalysis A: Gen,* 196 (2000) 1.

16. Z. Zhao and I. E. Wachs, Abstracts of papers, 222nd ACS National Meeting, Chicago, Aug., 2001.

17. P. Moriceau, B. Grzybowska, Y. Barbaux, G. Wrobel and G. Heequet, *Applied Catalysis,* 168 (1998) 269.

18. B. Grzybowska, J. Sloczynki, R. Grabowski, K. Wcislo, A. Kozlowska, J. Stock and J. Zielinski, *J. Catal.*, 178 (1998) 687.

19. S. De Rossi, G. Ferraris, S. Fremiotti, E. Garrone, G. Ghiotti, M.C. Campa and V. Indovina, *J. Catal.*, 148 (1994) 36.

20. F. Cavani, M. Koutyrev, F. Trifiro, A. Bartolini, D. Ghisletti, R. Iessi, A. Santucci and G. Delpiero, *J. Catal.*, 178 (1998) 687.

21. B. M. Weckhuysen and I. E. Wachs, *J. Phy. Chem.*, 100 (1996) 14437

22. M. Cherian, M. S. Rao, W. T. Wang, J. M. Jehng, A. M. Hirt and G. Deo, *Applied. Catalysis A: Gen.,* 233 (2002) 21-33.

23. M. Cherian, M. S. Rao, A. M. Hirt, I. E. Wachs and G. Deo, *J. Catal.*211,482-495 (2002)

24. J. Le Bras, J. C. Vedrine, A. Auroux, S. Trautmann and M. Baerns, *Applied Catalysis A: Gen.*, 88 (1992) 779.

25. M. J. Clement, A. Corma, S. Iborra and A. Velty, *J. Mol. Catal. A:Chem.*, 3475 (2002) 1.

26. M. Cherian, R. Gupta, M. S. Rao and G. Deo, *Catalysis Letters*, 86(4), 179 (2003)

27. B.Y. Jibril, S. M. Al- Zahrani and A.E. Abaseed, *Ind. Eng. Chem. Res.*, 39 (2000) 4070.

28. K. Kohler, J. Engweiler and A. Baiker, *J. Mol. Catal. A: Chem.*, 162 (2000) 423.

29. R.H.H. Smits, K. Seshan and J. R. H. Ross, in ACS Symposium Series, S. T. Oyama, J. W. Hightower, Eds. 1993, 523, 380

30. H. J. Hugo and J. H. Lunsford, *J. Catal.*, 91 (1985) 155.

31. O. F. Gorriz and L. E. Cadus, *Applied. Catalysis*, 180 (1999) 247.

32. G. Matra, F. Arena, S. Coluccia, F. Frusteri and A. Parmalina, *Catalysis Today*, 63 (2000) 197.

33. V. Ermini, E. Finocchio, S. Sechi, G. Busca and S. Rossini, *Applied. Catalysis A: Gen.*, 198 (2000) 67

34. K. Chen, S. Xie, A. T. Bell and E. Iglesia, *J. Catal.*, 195 (2000) 244.

35. A. A. Lemonidou, L. Nalabndian and I. A. Vasalos, *Catal. Today*, 61 (2000) 333.

36. J. Sloczynski, *Applied. Catalysis A: Gen.*, 146 (1996) 401.

37. R. Grabowski, B. Grzybowska, K. Samson, J. Sloczynski, J. Stoch and K. Wcislo, *Applied Catalysis A: Gen.*, 125 (1995) 129.

38. M. Ziyad, J. EL-Idrissi and M. Kacimi, *Catalysis Letters*, 56 (1998) 221.

39. O. Eduard and D. Vitaliy, Transactions of the Universities of Kosice (2002), (4), 46-51.

40. A. Maiti, N. Govind, P. Kung, D. King-Smith, J. E. Miller and C. Zhang, *Journal of Chemical Physics* (2002), 117(17), 8080-8088.

41. V. V Sidorchuk, V. M. Belousov, V. A. Zazhigalov, G. A.Komashko and A. I. Pyatnitskaya, Kataliz i Katalizatory (1987), 25 53-7. (Journal written in Russian)

42. M. Loukah, G. Coudurier,J. C. Vedrine and M. Ziyad, *Microporous Materials* (1995), 4(5), 345-58.

43. G. Ramis and G. Busca, *Catalysis Letters,* 18 (1993) 299.

44. G. Neri, A. Pistone, S. De Rossi, E. Rombi, C. Milone and S. Galvagno, *Applied Catalysis, A: General* (2004), 260(1), 75-86.

45. K. Chen, E. Iglesia and A. T. Bell, *J. Cat.* 192, 2000, 197.

46. K. Chen, A. Khodakov, J. Yang, A. T. Bell and E. Iglesia, *J. Catal., 186,* 1999, , 325

47. K. Chen, A. T. Bell and E. Iglesia, *J. Phys. Chem. B,* 104, 2000, 1292-1299.

48. D. Creaser, B. Andersson, R. R. Hudging, and P. L. Silveston, *The Canadian J. Chem. Engg.*, 78 (2000) 182.

49. D. Creaser and B. Andersson, *Applied catalysis,* 141 (1996) 131-152.

50. R. Grabowski, J. Sloczyñski and N. M. Grzesik, *Applied Catalysis A: General* 242 (2003) 297–309

51. A. Bottino, G. Capannelli, A. Comite, S. Storace and R. Felice, *Chemical Engineering Journal* 94 (2003) 11–18

52. G. F. Froment and K. B. Bischoff *Chemical Reactor Analysis and Design,* 2nd Edition, New York, 1990.

53. L. Elliott, S. D. Harris, D. B. Ingham and C.V. Wilson, *Compt. Methods Appl. Mech. Engg.*, 190 (2000) 1065-1095.

54. R. Moros, H. Kalies, H.G. Rex, and S. Schaffarczyk, *Computers & Chem. Engg.*, 20 (1996) 1257.

55. W. Polifke, W. Geng and K. Dobbeling, *Combust. Flame*, 113 (1998) 205.

56. K. Deb, *Optimization for Engineering Design,* Prentice-Hall of India Private Limited, 3rd Edition, New Delhi, 1998.

57. D.E. Goldberg, *Genetic Algorithm in Search, Optimization and Machine Learning,* Addision Wesley, Reading, MA, U.S.A. (1989).

58. J. H. Holland, *Adaption in Natural and artificial System,* University of Michigan Press, Ann Arbor, U.S.A. (1975).

59. G. Deo, I. E. Wachs and J. Haber, *Crit. Rev. Surf. Chem* , 4 (1994) 1.

60. G.E.P. Box, and N.R. Draper, *Biometrika,* 52 (1965) 355-365.

61. R. Mezaki and J.B. Butt, *I & EC fundamentals*, 7(1) (1968) 120-125.

62. S. Vajda, P. Valko, and A. Yermakova, *Computers and Chemical Engineering,* Vol. 10, No. 1 (1986) 49-58.

63. G. E. P. Box, W. G. Hunter, J. F. MacGregor, and J. Erjavec, *Technometrics*, Vol. 15, No.1, (1973) 33-51.

64. D. J. Pritchard and D. W. Bacon, *Chem. Eng. Sci.* 33 (1978) 1539

65. D. G. Watts, *J. Chem. Eng.* 72 (1994) 701.

66. V. Amte, *M. Tech Thesis*, IIT Kanpur, India, 1998.

67. S. V. Verma, *M. Tech Thesis.* IIT Kanpur, India, 1998.

68. A. Trunschke, D. L. Hoang, J. Radnik and H. Lieske, *J. Catal.*, 191 (2000) 456.

69. S. De Rossi, M.P. Casaletto, G. Ferraris, A. Cimino and G. Minelli, *Applied. Catalysis A: Gen.* 167 (1998) 257.

70. B. D. Raju, K.S.R. Rao, G.S. Selvapathi, P.S.S. Prasad and P.K. Rao, *Applied. Catalysis A: Gen.* 209 (2001) 335.

71. M. Zaki, N. Fouad, G. Bond and S. Tahir, *Thermochimica Acta* 285 (1996) 167-179.

72. M. Bertoldi, B. Fubini, E. Giamello, G. Busca, F. Trifiro and A. Vaccaria, *J. Chem. Soc. Faraday Trans.* 1, 84 (1988) 1405.

73. L. Forni and C. Oliva, *J. Chem. Soc., Faraday Trans.* 1, 84 (1988) 2477.

74. A. Chimino, D. Gordischi, S. De Rossi, G. Ferrars, D. Gazzoli, V. Indovina, G. Minelli, M. Occhiuzzi and M. Valligi, *J. Catal.*, 127 (1991) 761.

75. K. Kohler, C. W. Schlapfer, A. von Zelewsky, J. Nickl, J. Engweiler and A. baiker, *J. Catal.* 127 (1991) 761.

76. S. Khadder-Zine, A. Ghorbel and C. Naccache, *J. Mol. Catal.* , 150 (1999) 223.

77. H. Scott Fogler, *Elements Of Chemical Reaction Engineering*, Prentice-Hall of India Private Limited, 3rd Edition, New Delhi, 2002

Appendix-1

Raw Peak Areas obtained in Contact Time Studies

Table A-1.1 Raw Peak Areas obtained in the contact time study of 3CrTi catalyst.

Weight of the catalyst = 0.1 g; Temperature = 653 K; Propane: Air=2:1.

Total Flow Rate (cc/min)	Contact Time (kg $m^{-3}s$)	Raw Areas			
		C_3H_8	C_3H_6	CO_2	CO
120	50	1813.843	2.989	4.454	2.049
120	50	1815.875	2.920	4.269	1.877
90	70	1875.932	3.542	5.205	2.309
90	70	1874.602	3.500	5.387	2.480
75	80	1789.086	3.761	6.353	2.491
75	80	1756.879	3.775	6.650	2.523
45	130	1770.500	4.255	9.131	3.354
45	130	1774.844	4.520	8.302	3.301
30	200	1637.594	5.007	10.955	4.105
30	200	1744.080	5.452	11.550	4.981
20	300	1697.442	6.576	15.250	5.637
20	300	1841.882	7.078	17.011	6.027

Table A-1.2 Raw Peak Areas obtained in the contact time study of 2Cr1PTi catalyst.

Weight of the catalyst = 0.2 g; Temperature = 653 K; Propane: Air =2:1.

Total Flow Rate (cc/min)	Contact Time (kg $m^{-3}s$)	Raw Areas			
		C_3H_8	C_3H_6	CO_2	CO
75	160	1465.550	3.471	3.342	1.412
75	160	1460.524	3.321	2.989	1.012
60	200	1438.330	4.085	3.660	1.740
60	200	1467.040	3.835	3.577	1.684
45	270	1385.420	4.561	4.461	1.942
45	270	1350.102	4.213	4.587	2.014
30	400	1345.750	5.675	5.624	2.831
30	400	1330.425	5.560	5.501	2.534

Table A-1.3 Raw Peak Areas obtained in the contact time study of 1.5Cr1PTi catalyst. Weight of the catalyst = 0.2 g; Temperature = 653 K; Propane: Air =2:1.

Total Flow Rate (cc/min)	Contact Time (kg $m^{-3}s$)	Raw Areas			
		C_3H_8	C_3H_6	CO_2	CO
120	100	1355.740	5.157	2.286	1.371
120	100	1423.050	3.510	1.730	0.886
90	130	1473.610	3.990	1.969	1.039
90	130	1626.545	4.010	2.204	1.222
75	160	1515.892	3.943	1.986	1.112
75	160	1463.640	3.676	1.981	1.127
45	270	1463.790	4.586	2.969	1.489
45	270	1448.164	4.851	2.847	1.525
30	400	1404.390	5.719	3.642	1.874
30	400	1418.528	6.609	4.189	2.195
20	600	1371.710	8.531	5.462	2.683
20	600	1371.836	8.362	5.208	2.728

Table A-1.4 Raw Peak Areas obtained in the contact time study of 1Cr1PTi catalyst. Weight of the catalyst = 0.2 g; Temperature = 653 K; Propane: Air =2:1.

Total Flow Rate (cc/min)	Contact Time (kg $m^{-3}s$)	Raw Areas			
		C_3H_8	C_3H_6	CO_2	CO
120	100	1584.510	2.481	1.374	0.924
120	100	1560.964	2.670	2.170	1.028
90	130	1535.718	2.910	2.018	1.158
90	130	1540.741	3.141	1.654	0.954
75	160	1545.165	3.502	2.275	1.169
75	160	1580.990	3.536	2.453	1.258
45	270	1494.786	4.148	3.268	1.643
45	270	1500.742	4.056	3.158	1.548
30	400	1582.866	5.165	3.641	1.741
30	400	1522.866	4.889	3.841	2.048
20	600	1535.718	5.904	2.018	1.158
20	600	1500.982	5.748	1.985	1.425

Appendix-2

Table A-2.1 Raw Peak Areas obtained in Propane ODH reaction study for 3CrTi catalyst

Weight of the catalyst = 0.2 g; Total flow rate =75cc/min.

C_3H_8/O_2 ratio	Zero Area	Reaction Temperature (K)	Raw Areas			
			C_3H_8	C_3H_6	CO_2	CO
1:1	**555**	**633**	**552.588**	**2.729**	**11.261**	**2.149**
		633	555.030	3.240	10.435	1.843
		653	**537.534**	**7.721**	**23.592**	**5.201**
		653	536.936	7.846	23.076	5.037
		673	501.198	21.854	59.267	19.370
		673	505.790	17.015	46.778	14.511
2:1	**1280**	**633**	**1255.146**	**3.824**	**22.904**	**3.356**
		633	1260.799	3.542	20.394	3.174
		653	**1254.294**	**9.182**	**37.826**	**6.784**
		653	1260.453	9.338	41.002	7.417
		673	**1260.831**	**16.740**	**50.136**	**11.934**
		673	1273.408	16.795	48.213	11.510
3:1	**1442**	**633**	**1405.301**	**7.317**	**29.389**	**7.025**
		633	1427.512	4.940	20.948	6.681
		653	**1426.402**	**27.087**	**56.658**	**19.368**
		653	1410.054	23.226	43.326	16.633
		673	**1372.779**	**34.176**	**57.567**	**23.607**
		673	1362.297	40.128	56.889	26.231

* The values used in the study are marked as bold.

Table A-2.2 Raw Peak Areas obtained in Propane ODH reaction study for 2Cr1PTi catalyst

Weight of the catalyst = 0.2 g; Total flow rate =75cc/min.

C_3H_8/O_2 ratio)	Zero Area	Reaction Temperature (K)	Raw Areas			
			C_3H_8	C_3H_6	CO_2	CO
1:1	340	**633**	**327.838**	**0.785**	**2.341**	**0.649**
		633	338.846	0.761	2.179	0.611
		653	**333.402**	**1.428**	**3.761**	**1.06**
		653	338.797	1.453	3.953	1.077
		673	**331.327**	**2.451**	**5.729**	**1.763**
		673	337.075	2.634	5.638	1.778
2:1	1300	**633**	**1280.757**	**2.929**	**5.652**	**1.934**
		633	1298.87	3.782	7.097	2.488
		653	**1275.053**	**7.685**	**15.097**	**4.597**
		653	1270.368	7.801	15.605	4.623
		673	**1243.273**	**18.593**	**31.797**	**10.327**
		673	1236.435	14.912	23.816	8.092
3:1	1450	**633**	**1437.919**	**3.195**	**4.635**	**1.708**
		633	1424.675	3.007	4.167	1.682
		653	**1439.016**	**6.398**	**9.995**	**3.542**
		653	1425.007	6.600	10.046	3.615
		673	**1415.524**	**17.232**	**25.148**	**9.136**
		673	1413.159	16.901	23.028	8.286

* The values used in the study are marked as bold.

Table A-2.3 Raw Peak Areas obtained in Propane ODH reaction study for 1.5Cr1PTi catalyst

Weight of the catalyst = 0.2 g; Total flow rate =75cc/min.

C_3H_8/O_2 ratio)	Zero Area	Reaction Temperature (K)	Raw Areas			
			C_3H_8	C_3H_6	CO_2	CO
1:1	760	**633**	**751.730**	**1.333**	**3.132**	**0.740**
		633	758.900	1.204	3.275	0.957
		653	**741.316**	**2.663**	**5.967**	**1.778**
		653	751.404	2.730	8.108	1.955
		673	**617.690**	**3.924**	**9.990**	**2.994**
		673	610.255	3.320	8.698	2.586
2:1	1080	**633**	**1045.534**	**2.311**	**3.433**	**1.029**
		633	1044.583	2.499	3.522	1.205
		653	**1032.925**	**2.903**	**3.603**	**1.543**
		653	1016.221	3.918	5.848	1.976
		673	**1022.888**	**9.009**	**13.440**	**4.824**
		673	1017.346	8.476	12.070	4.448
3:1	1960	**633**	**1888.488**	**4.529**	**5.353**	**2.088**
		633	1949.125	4.926	5.799	2.261
		653	**1846.969**	**8.697**	**11.333**	**4.002**
		653	1886.337	9.081	12.585	4.313
		673	**1838.803**	**17.714**	**21.859**	**7.712**
		673	1823.903	18.108	23.367	8.416

* The values used in the study are marked as bold.

Table A-2.4 Raw Peak Areas obtained in Propane ODH reaction study for 1Cr1PTi catalyst

Weight of the catalyst = 0.2 g; Total flow rate =75cc/min.

C_3H_8/O_2 ratio)	Zero Area	Reaction Temperature (K)	Raw Areas			
			C_3H_8	C_3H_6	CO_2	CO
1:1	600	**633**	**595.735**	**1.542**	**3.624**	**0.384**
		633	588.081	1.414	3.525	0.37
		653	**585.086**	**2.134**	**6.762**	**0.411**
		653	589.716	2.290	6.409	0.445
		673	**579.551**	**2.966**	**12.367**	**0.747**
		673	597.328	2.867	12.454	0.722
2:1	765	**633**	**751.151**	**0.851**	**0.664**	**0.265**
		633	748.965	0.831	0.666	0.246
		653	**734.224**	**1.815**	**1.429**	**0.545**
		653	759.245	1.887	1.577	0.668
		673	**726.647**	**2.921**	**2.118**	**0.969**
		673	712.654	2.883	2.016	0.928
3:1	1950	**633**	**1945.708**	**1.516**	**1.389**	**0.419**
		633	1925.895	1.305	1.312	0.435
		653	**1880.649**	**2.495**	**2.149**	**0.802**
		653	1881.576	2.578	1.924	0.715
		673	**1732.371**	**4.417**	**3.173**	**1.355**
		673	1711.762	4.66	3.467	1.361

* The values used in the study are marked as bold.

Appendix-3

TABLE A-3.1: Input and output mole percentages for 3CrTi catalyst

Weight of the catalyst = 0.2 g; Total flow rate =75 cc/min

Temperature (K)	Input mole (%)		Output mole (%)			
	C_3H_8	O_2	C_3H_8	C_3H_6	CO_2	CO
633	17.355	17.355	17.051	0.049	0.208	0.042
653	17.355	17.355	16.229	0.153	0.504	0.112
673	17.355	17.355	15.204	0.331	0.833	0.283
633	29.577	14.789	29.289	0.039	0.322	0.047
653	29.577	14.789	28.876	0.111	0.597	0.109
673	29.577	14.789	28.729	0.228	0.732	0.192
633	38.650	12.883	38.363	0.034	0.231	0.040
653	38.650	12.883	38.126	0.073	0.428	0.081
673	38.650	12.883	37.062	0.281	0.685	0.235

TABLE-A-3.2: Input and output mole percentages for 2Cr1PTi catalyst

Weight of the catalyst = 0.2 g; Total flow rate =75 cc/min

Temperature (K)	Input mole (%)		Output mole (%)			
	C_3H_8	O_2	C_3H_8	C_3H_6	CO_2	CO
633	17.355	17.355	17.724	0.042	0.104	0.029
653	17.355	17.355	17.439	0.078	0.180	0.051
673	17.355	17.355	17.330	0.134	0.274	0.084
633	29.577	14.789	29.515	0.082	0.121	0.042
653	29.577	14.789	29.235	0.185	0.317	0.097
673	29.577	14.789	28.349	0.356	0.500	0.17
633	38.650	12.883	38.470	0.089	0.114	0.042
653	38.650	12.883	38.124	0.185	0.245	0.089
673	38.650	12.883	37.871	0.483	0.616	0.224

TABLE-A-3.3: Input and output mole percentages for 1.5Cr1PTi catalyst

Weight of the catalyst = 0.2 g; Total flow rate =75 cc/min

Temperature (K)	Input mole (%)		Output mole (%)			
	C_3H_8	O_2	C_3H_8	C_3H_6	CO_2	CO
633	17.355	17.355	17.258	0.032	0.066	0.016
653	17.355	17.355	17.019	0.064	0.125	0.037
673	17.355	17.355	14.181	0.094	0.210	0.063
633	29.577	14.789	29.013	0.067	0.087	0.026
653	29.577	14.789	28.663	0.084	0.092	0.039
673	29.577	14.789	28.384	0.262	0.342	0.123
633	38.650	12.883	38.416	0.096	0.099	0.039
653	38.650	12.883	37.572	0.185	0.211	0.075
673	38.650	12.883	37.405	0.378	0.407	0.144

TABLE-A-3.4: Input and output mole percentages for 1Cr1PTi catalyst

Weight of the catalyst = 0.2 g; Total flow rate =75 cc/min

Temperature (K)	Input mole (%)		Output mole (%)			
	C_3H_8	O_2	C_3H_8	C_3H_6	CO_2	CO
633	17.355	17.355	17.129	0.047	0.096	0.009
653	17.355	17.355	17.085	0.070	0.170	0.012
673	17.355	17.355	17.080	0.090	0.328	0.020
633	29.577	14.789	28.047	0.113	0.069	0.032
653	29.577	14.789	27.818	0.072	0.054	0.021
673	29.577	14.789	27.132	0.114	0.072	0.033
633	38.650	12.883	38.248	0.029	0.022	0.008
653	38.650	12.883	37.288	0.052	0.033	0.011
673	38.650	12.883	35.521	0.093	0.059	0.025

Appendix-4

Table 4.7: Kinetic-parameters for PL-2 Model

Calculated at $P_{m(C_3H_8)}$ = 0.2958 atm, $P_{m(O_2)}$ = 0.148 atm, T_m = 653.16 K

Parameter	Units	Catalyst			
		3CrTi	2Cr1PTi	1.5Cr1PTi	1Cr1PTi
k_{10}	$ml\ STP\ min^{-1}\ (g\ cat)^{-1}\ atm^{-(a1+b1)}$	0.99	0.69	0.50	0.18
k_{20}		0.33	0.13	0.07	0.03
k_{30}		2.16	0.47	0.22	0.26
E_1	$kJ\ mol^{-1}$	183	140	142	110
E_2		136	125	117	97
E_3		106	102	124	130
a_1	*Dimensionless*	0.28	1.0	1.0	0.01
b_1		1.0	0.35	0.01	1.0
a_2		0.01	0.6	1.0	0.26
b_2		0.27	0.01	1.0	1.0
a_3		0.22	0.65	0.49	0.01
b_3		1.0	1.0	0.40	1.0